REPORT DOCUMENTATION PAGE

AFRL-SR-AR-TR-03-

0192

1. REPORT DATE *(DD-MM-YYYY)* 07-05-03	2. REPORT TYPE FINAL	3. DATES COVERED *(From - To)* 01-dec-99 - 31-jan-03
4. TITLE AND SUBTITLE Final Report-Frontier Geoplasma Research		5a. CONTRACT NUMBER
		5b. GRANT NUMBER F 49620-00-1-0004
		5c. PROGRAM ELEMENT NUMBER
6. AUTHOR(S) Tom Chang	05-13-03A06:39 RCVD	5d. PROJECT NUMBER
		5e. TASK NUMBER
		5f. WORK UNIT NUMBER
7. PERFORMING ORGANIZATION NAME(S) AND ADDRESS(ES) MIT	37-271, 77 Massachusetts Avenue Cambridge MA 02139	8. PERFORMING ORGANIZATION REPORT NUMBER
9. SPONSORING / MONITORING AGENCY NAME(S) AND ADDRESS(ES) Air Force Office of Scientific Research/NM	4015 Wilson Boulevard, Rm. 732 Arlington VA 22203-1954	10. SPONSOR/MONITOR'S ACRONYM(S) AFOSR/NM
		11. SPONSOR/MONITOR'S REPORT NUMBER(S)

12. DISTRIBUTION / AVAILABILITY STATEMENT

Approved for public release;
Distribution unlimited

20030604 060

13. SUPPLEMENTARY NOTES

14. ABSTRACT

The Center for Theoretical Geo/Cosmo Plasma Physics was established by the Air Force Office of Scientific Research in 1986 through a DoD University Research Initiative (URI) Grant via keen national competition. The goal of the center since its inception has been to develop and maintain a program of excellence in interdisciplinary space plasma research involving the mutual interactions of collaborating members of a select group of space scientists, plasma physicists, mathematicians and numerical analysts. During the past several years, under the grant title, "Frontier Geoplasma Research", members of the center have made seminal contributions to a number of definitive research findings related to the phenomena of intermittent plasma turbulence, forced and/or self-organized criticality, global acceleration of the solar wind and polar wind, sporadic localized reconnections in the magnetotail and in the auroral zone, charged particle energization through wave-particle interactions, the black auroral curls, multi-scale evolutions, magnetosphere/ionosphere coupling, and the theory of complexity in space plasmas. Some of the results of these research activities have already found practical applications toward the missions of the United States Air Force, primarily through the collaborating efforts between the center members and members of the research group headed by Dr. J.R. Jasperse at the Air Force Research Laboratory.

15. SUBJECT TERMS

Theoretical Geoplasma Physics

16. SECURITY CLASSIFICATION OF:			17. LIMITATION OF ABSTRACT	18. NUMBER OF PAGES	19a. NAME OF RESPONSIBLE PERSON Dr. Paul J. Bellaire, Jr. MajorUS
a. REPORT unclassified	b. ABSTRACT unclassified	c. THIS PAGE unclassified	unlimited unclassified	91	19b. TELEPHONE NUMBER *(include area code)* 703-696-8411

Standard Form 298 (Rev. 8-98)
Prescribed by ANSI Std. Z39.18

05-13-03A06:39 RCVD

Final Report Submitted to the

Air Force Office of Scientific Research

FRONTIER GEOPLASMA RESEARCH

Performed under Grant Number
F49620-00-1-0004

For the Attention of
Major Paul J. Bellaire, Jr., Ph.D.
Program Manager, Space Sciences
Air Force Office of Scientific Research, AFOSR/NM
4015 Wilson Boulevard, Rm. 732
Arlington, VA 22203-1954

Submitted by the
Center for Theoretical Geo/Cosmo Plasma Physics
Massachusetts Institute of Technology
Cambridge, MA 02139

Tom T.S. Chang
Director and Principal Investigator
Tel: 617-2537523
Fax: 617-2530861
Email: tsc@space.mit.edu

May 2003

TABLE OF CONTENTS

I. ABSTRACT

The Center for Theoretical Geo/Cosmo Plasma Physics was established by the Air Force Office of Scientific Research in 1986 through a DoD University Research Initiative (URI) Grant via keen national competition. The goal of the center since its inception has been to develop and maintain a program of excellence in interdisciplinary space plasma research involving the mutual interactions of collaborating members of a select group of space scientists, plasma physicists, mathematicians and numerical analysts. During the past several years, under the grant title, "Frontier Geoplasma Research", members of the center have made seminal contributions to a number of definitive research findings related to the phenomena of intermittent plasma turbulence, forced and/or self-organized criticality, global acceleration of the solar wind and polar wind, sporadic localized reconnections in the magnetotail and in the auroral zone, charged particle energization through wave-particle interactions, the black auroral curls, multi-scale evolutions, magnetosphere/ionosphere coupling, and the theory of complexity in space plasmas. Some of the results of these research activities have already found practical applications toward the missions of the United States Air Force, primarily through the collaborating efforts between the center members and members of the research group headed by Dr. J.R. Jasperse at the Air Force Research Laboratory.

The MIT Center is now recognized by their peers worldwide as a star example of a successful enterprise between a prestigious educational institution and an established governmental research laboratory, the Air Force Research Laboratory [AFRL]. In addition to our collaborating research efforts, our center and AFRL have co-sponsored a symposium series on the "Physics of Space Plasmas" and a workshop series on

"Theoretical Geoplasma Physics", now under the combined name, the "Cambridge Symposia/Workshops on Space Plasma Physics". The center also periodically co-sponsors other scientific workshops and symposia with other institutions on various important topics of current space plasma research. Proceedings of these symposia and workshops have become important research resources for these current topics. For example, one such recent volume was devoted to the memory of Professor Subrahmanyan Chandrasekhar, a Nobel laureate and a giant in the scientific fields of plasma physics, astrophysics and space sciences. Other noteworthy contributions include the volume of a collection of outstanding contributions in the modern physics of complexity published as a special issue entitled "Forced and/or Self-Organiced Criticality [FSOC] in Space Plasmas" by the Journal of Atmospheric and Solar Terrestrial Physics [JASTP], and a special topics section on Transports Processes in Geospace in the journal of Plasma Physics.

The center has participated actively with the graduate school of MIT, in a Minority Summer Research Program, to effect changes in the realm of graduate scientific training for minorities. It is also an active participant in the Research Scientist Institute (RSI) program with the Washington-based Center of Excellence in Education (CEE) in sponsoring the preparation of genius-level high school students recruited worldwide in preparation for them to achieve the ultimate of their capabilities. CEE was founded by Admiral Rickover in 1983 and its honorary trustees include such luminaries as former president Jimmy Carter, Senator Joseph Leiberman, and Secretary Colin Powell. In addition, the MIT center has maintained an active visiting scientists program, which has kept our research program vibrant and up-to-date.

During the period, the members of the center have published 24 scientific papers, books and proceedings, and have been invited to deliver 27 invited and review lectures at various international conferences and renowned educational and research institutions.

II. INTRODUCTION

For the United States Air Force to enjoy its continuing success in meeting the demands of its mission heading into the 21st century, it must be prepared to operate in the "New Frontiers" of space, particularly its ever-changing turbulent geoplasma environment. Recognizing this importance, a Center of Excellence in Theoretical Geo/Cosmo Plasma Physics was established (through keen national competition) at the Massachusetts Institute of Technology under the sponsorship of the Air Force Office of Scientific Research.

Benefiting from strong interactions with the members of the Air Force Research Laboratory at Hanscom, MA, our Center has made substantive progress toward the goals set forth since its inception. The close proximity between the two institutions has allowed direct personnel exchanges as well as direct and meaningful collaborations in numerous relevant research programs in geoplasma physics. During the past few years, under the grant name, "Frontier Geoplasma Research", we have succeeded in jointly developing the fundamental understanding of several multiscale space plasma phenomena of cutting-edge importance. These include the study of the origin of broad-band low frequency turbulence in the auroral zone and the associated wave-particle interactions such as the anomalous acceleration of ionospheric oxygen ions into magnetospheric energies, the global acceleration and evolution of fast solar streams into the distant helisphere, the generation of intense divergent electric fields and the phenomena of black auroral curls, the self-consistent kinetic evolution and the dynamic understanding of the day-night asymmetry of photoelectron-driven polar winds, the onset of coherent structures and associated double layers in the acceleration region of the

ionosphere, the study of intermittent turbulence and sporadic localized reconnections in the Earth's magnetotail and the solar wind, the formation of ion conics and counter-streaming electrons along auroral field lines, and the general phenomena of complexity involving the coupling of the ionosphere, magnetosphere, and the solar wind. Together, we have published (during the past several years) 24 joint technical papers and books, and delivered 27 invited and review lectures at various international conferences and renowned institutions.

A number of the afore-mentioned research findings have already found practical applications by our colleagues at the Air Force Research Laboratory. Examples of such applications are: the prediction of charged-particle precipitation patterns and deposition profiles in the diffuse-auroral zone of the ionosphere, the prediction of solar EUV and X-ray fluxes based on the ionospheric photoelectron measurements and transport calculations, the calculation of ionospheric electron density profiles in the equatorial, mid-, and high-latitude portions of the globe and associated local, nonlocal, and nonlinear instabilities, and a fully self-consistent analytical model that is capable of accurately predicting the various features of the turbulent geoplasma environment (particularly in the downward auroral current regions) relevant to important Air Force operations.

Our Center and the Air Force Research Laboratory (led by Drs. Tom Chang at MIT and J.R. Jasperse at AFRL) jointly inaugurated a series of symposia on the "Physics of Space Plasmas". The original purpose of these symposia is to provide an annual get-together for space scientists in the Boston-New England area. Its coverage has since attracted contributions from scientists worldwide. Each symposium included the presentation of an "Alfven lecture" established in honor of the Nobel Laureate, Professor

Hannes Alfven of the Swedish Royal Institute of Technology. Professor Alfven has strongly supported the activities of the MIT center. He was a founding honorary member of the center and visits the center often during its formative years. Alfven Lecturers have included such luminaries as Professor Oscar Buneman of the Stanford University, Professor Jim Dungey of the Imperial College, London, Professor Eugene Parker of the University of Chicago, Dr. Roger Gendrin of the French National Laboratory of Ionospheric and Magnetospheric Physics, Professor James van Allen of the University of Iowa, Professor Charles Kennel of UCLA and the Scripps Institution (and a former Associate Administrator of NASA), and Professor Alfven himself who inaugurated the series.

Jointly with AFRL, we also organized a series of workshops in "Geoplasma Research". Each workshop was targeted at a specific topic of frontier geoplasma physics and includes basic tutorial talks and invited specialty lectures. The format of the workshops has been designed to allow ample discussion time and individual interactions. Since the untimely passing of Professor Alfven, we have combined the symposium-workshop activities into a single series entitled: the "Cambridge Symposia/Workshops on Space Plasma Physics". During our recent 15th Cambridge Symposium/Workshop held in Cascais, Portugal, Professor Carl-Gunne Falthammar of the Royal Institute of Technology and the Alfven Laboratory of Plasma Physics, a favorite student of Professor Alfven, was the first Alfven Memorial Lecturer of the new series. Such activities have received much praise from the worldwide geo/cosmo community. Proceedings of the series entitled, "Physics of Space Plasmas", have become informal textbooks treasured by both established scientists and students in geo/cosmo research. . The center also

periodically co-sponsors other scientific workshops and symposia with other institutions on various important topics of current space plasma research. One such recent volume was devoted to the memory of Professor S. Chandrasekhar of the University of Chicago. Professor Chandrasekhar, a Nobel laureate, was a giant in the scientific fields of plasma physics, statistical mechanics, astrophysics and space sciences, radiative transfer, and MHD stability. This memorial volume covers the entire spectrum of "Chandra's" research interests. Other noteworthy contributions by the center include the editing of the collection of a set of outstanding contributions by a group of international scientists whose specialty are in the physics of complexity in a special issue entitled "Forced and/or Self-Organiced Criticality [FSOC] in Space Plasmas" published by the Journal of Atmospheric and Solar Terrestrial Physics [JASTP], and a Special Topics Section on Transport Processes in Geospace in the journal of Plasma Physics.

Our center has interacted actively with a number or research organizations and universities in addition to the Air Force Research Laboratory. These include, the International Space Science Institute in Bern, Switzerland, the Italian National Space Research Institute in Rome, the Institute of Space and Astronautical Science, Japan, the University of Calgary, Canada, the Applied Physics Laboratory of the Johns Hopkins University, the Max-Planck Institutes for Extraterrestrial Physics and Aeronomy in Germany, the Lockheed-Martin Palo Alto Research Laboratory, the Universities of California at Berkeley, Los Angeles and Irvine, the Cornell University, the University of New Hampshire, NASA Goddard Space Flight Center, the National Research Council of Canada, the Naval Research Laboratory, the Imperial College of London, the University of Warwick, England, the British Antarctic Survey, Boston College and the Boston

University. Visits to these institutions and by scientists from these institutions have provided the necessary stimulus to keep our research program vibrant, up-to-date, and at the same time constantly in touch with practical applications.

One of the prime missions of the MIT Center for Theoretical Geo/Cosmo Plasma Physics is to provide an environment for the development of young prospective students in space plasma education. During the past several years, in cooperation with the MIT Graduate School and the MIT Minority Summer Research Program (MSRP), our center hosted a number of talented young minority and female undergraduate interns. By intermingling with the established scientists at the center, these young interns obtained first hand knowledge of the true meaning of cutting-edge scientific research in space physics. The MIT Center also played an active role in the Research Scientist Institute (RSI) program in collaboration with the Washington-based Center of Excellence in Education (CEE) in sponsoring the education of genius-level high school students recruited worldwide in preparation for them to achieve the ultimate of their scientific capabilities. CEE was founded by Admiral Rickover in 1983 and its honorary trustees include such luminaries as former president Jimmy Carter, Senator Joseph Leiberman, and General Colin Powell. RSI alumni have dominated all scholarship competitions of national talent search programs and many have become leaders in the various fields of the 21st century cutting-edge scientific disciplines.

This report is organized as follows: In Sec. III, we discuss the progress of our center by including sub-sections of detailed descriptions of two of our recent major accomplishments, followed by a complete list of the center research topics. In Section IV, we provide a complete list of scientific publications by members affiliated with the

Center. A complete list of invited and review lectures by the center personnel given at various conferences, meetings, and research institutions is given in Section V. Finally, a list of the past and present center personnel is given in Sec. VI.

III. PROGRESS AND ACCOMPLISHMENTS

In our original AFOSR URI proposal, we proposed a unique program of theoretical research in geoplasma physics. The Center would be a single cohesive unit of scientists from several disciplines interacting effectively with one another and with groups from external ongoing experimental research programs. It would not be the purpose of the Center to carry out routine data analyses. Instead, our approach would be to interact with the experimental groups and to identify from the analyzed data those problems that had no ready-made explanations and to focus our efforts on the solution of such new problems. At all times, we would not lose sight of the practical applications of the developed theories to the prime mission of the Air Force.

During the past few years under the current grant program "Frontier Geoplasma Research", we have endeavored to follow such guidelines while developing the various research efforts at the Center. We identified many new, interesting, and at the same time puzzling geoplasma problems that were not admissible to "routine" solutions. We have provided theoretical understanding to a number of such identified problems. In many of these instances, we were able to provide quantitative descriptions of the phenomena or make useful theoretical predictions for future observations and applications.

The most exciting research findings of our group during this period included the development of a first truly kinetic theory of the global evolution of the fast stream solar wind including the wave-particle energization of the ions and electrons, an "Intermittent Turbulence Theory" of sporadic localized magnetic reconnections that is germane to the coupling process between the ionosphere and magnetosphere in the auroral region and in the dynamics of the plasma sheet of the Earth's magnetotail and the solar wind, the

anomalous energization of ionospheric ions in the acceleration and reverse-current regions of the auroral zone, and the development of a novel theory of the photoelectron-driven polar wind based on the kinetic and anomalous heat transport of the field-aligned electrons, and nonthermal ions in the dayside polar ionosphere. We have included below two sub-sections to describe the details and seminal aspects of these research results.

Other important research activities of the center included: the study of the dynamics of the coherent structures such as double layers and fast electron holes in the ionosphere, the dynamics of upward propagating lightning strokes, the multi-dimensional aspects of the black auroral curls, the development and propagation of electromagnetic ion cyclotron waves throughout the terrestrial ionosphere, and various processes related to the coupling of the ionosphere and magnetosphere.

A number of our research findings have recently been confirmed by the experimental data collected by high-time resolution instruments on board the FREJA, VIKING, POLAR, DE, FAST and "AKEBONO" satellites as well as the TOPAZ, SCIFER, AMICIST, and other high-altitude rockets. As it has been the history of all past research activities of the MIT Center, our recent work is directly related to AF C^3I systems. The coupling phenomenon between the Earth's ionosphere and magnetosphere, intermittent MHD turbulence, the polar wind outflow, the black auroral curls, and ionospheric lower hybrid cavitary structures all have profound effects on the high-latitude electron and ion density profiles as well as signal and wave propagations. The understanding of these phenomena is germane to space surveillance, space launch and orbit operations, as well as space weather modeling and forecasting. In particular, our understanding of pitch-angle scattering and the dynamics of the central plasma sheet

allowed us to construct a quantitative model of electron precipitation in the diffuse aurora. Because this precipitation helps control the electron density profile in the high-latitude ionosphere, it has a strong impact on the Air Force communication and surveillance systems that must operate in the region. Similarly, because of the effect of scintillation on these systems and the close relationship between scintillations and the high-latitude ionospheric turbulence, our quantitative models of the latter phenomena and its consequences can be expected to have great utility in the practical business of ionospheric weather prediction.

Listed below are research topics that have been studied and analyzed by the members of the center personnel during the grant period followed by the two subsections on the solar wind, self-organized criticality, ion acceleration, intermittent turbulence and complexity.

- Anisotropic, intermittent turbulence in the solar wind.
- Sporadic, localized magnetic reconnection and intermittent turbulence in the ionosphere-magnetosphere coupling region and in the Earth's magnetotail.
- Ion heating by low frequency waves in Earth's ionosphere and magnetosphere.
- Kinetic theory of the global evolution of the fast stream solar wind including the wave-particle energization of the ions and electrons.
- Lower hybrid collapse, caviton turbulence, and charged particle energization in the topside ionosphere.
- Mode conversion processes involving the plasma turbulence of oxygen-hydrogen plasmas in the magnetosphere and ionosphere.
- Anisotropic, kinetic polar wind driven by the dayside-photoelectrons.

- Nonlinear vortex description of black auroral curls.
- Turbulent relaxation of magnetic fields in space plasmas.
- Ion and electron acceleration along auroral field lines.
- Nonlocal effects of finite beam-driven instabilities in space plasmas.
- Path integral approach to nonlinear particle acceleration and diffusion in ionospheric plasmas.
- Convection of ion cyclotron waves to ion heating regions.
- Broad-band spectrum of auroral plasma turbulence.
- Renormalization-group calculation of self-organized criticality and low-dimensional behavior of auroral substorm onsets.
- Theory of nonlinear electric fields in the auroral acceleration region.
- Stochastic MHD models for space plasmas.
- Multiple-cyclotron absorption of ion heating in the cusp/cleft region.
- Wave-particle ion cyclotron turbulence and evolution of the electron distribution in inhomogeneous space plasmas.
- ULF waves along auroral field lines in the central plasma sheet.
- Energy source and generation mechanism for auroral kilometric radiation.
- Upward propagating intense lightning strokes and associated infrared emissions in the lower ionosphere.
- Particle acceleration by intense auroral VLF waves.
- The electron beam instability and turbulence theories in space plasmas.
- Two stream interaction on auroral field lines.

- Energetic photoelectron and the polar rain.
- Monte-Carlo modeling of polar wind electron distributions with anomalous heat flux.
- Counterstreaming electrons generated by lower hybrid waves in the auroral region.
- Heating of thermal ions near the equatorward boundary of the mid-altitude polar cusp.
- Stabilization of the cyclotron autoresonance maser instability in space plasmas.
- Nonlinear oblique whistler modes in collisionless shocks of space plasmas.
- Electromagnetic tornadoes in space.
- Radiations from large space structures in low Earth orbit with induced AC currents.
- Ion waves and upgoing ion beams observed by the VIKING satellite.
- Simulation of ion conic formation in the ionosphere and magnetosphere.
- Alfvén engine in space.
- Convection of ion cyclotron waves to ion heating regions in the auroral zone.
- Wave observations and their relation to nonresonant and resonant particle heating processes.

III.1 Complexity, Forced and/or Self-Organized Criticality, and Topological Phase Transitions in Geospace Plasmas -- A Challenge To High-Speed Computing and Numerical Simulation

III.1.1 Introduction

Research activity in geospace plasma physics is now arriving at an interesting juncture that becomes apparent when looking back at what has been accomplished in the past and looking forward to what will be required in the next decade. In this regard, it is noted that considerable observational and theoretical attention has been devoted towards the understanding of local, point observations of geospace plasma phenomena as they have been identified on US/European/Japanese research satellites. However, it is becoming clear that important questions that will be receiving attention in the coming years (particularly with the successful launches of the CLUSTER II and IMAGE satellites) are addressed toward global and multiscale issues: questions of energy and momentum transport within the magnetosphere, ionosphere and the Sun-Earth connection region, and of the nature of the particle populations, their source, entry, energization, diffusion, and ultimate loss from the systems. Thus, observations are becoming multi-spacecraft and/or multi-point in scope, and theoretical models are likewise being forced to confront issues of nonlocality and "complexity".

In this review, we discuss a number of such geospace plasma processes of complexity, with special emphasis on the dynamics of the magnetotail and its substorm behavior. We demonstrate that the sporadic and localized interactions of magnetic coherent structures arising from plasma resonances are the origin of "complexity" in geospace plasmas. Such interactions, which generate the anomalous diffusion, transport

and evolution of the macroscopic state variables of the overall dynamic system, may be modeled by a triggered localized chaotic growth equation of a set of relevant order parameters. The dynamics of such intermittent processes would generally pave the way for the global system to evolve into a "complex" state of long-ranged interactions of fluctuations, displaying the phenomenon of forced and/or self-organized criticality (FSOC). The coarse-grained dissipation due to the intermittent fluctuations can also induce "fluctuation-induced nonlinear instabilities" that can, in turn, reconfigure the topology of background magnetic fields.

The organization of this paper is as follows. In Section III.1.2, we discuss the origin of the stochastically distributed coherent magnetic structures in the Earth's magnetotail. In Section III.1.3, we consider the preferential acceleration of the coherent magnetic structures in the neutral sheet region and their relevance to the interpretation of the observed fast bursty bulk flows (BBF). In Section III.1.4, we consider the localized merging processes of the coherent structures and their connection to the observed localized, sporadic reconnection signatures in geoplasmas (e.g., in the Earth's magnetotail). The concept and implications of the phenomenon of FSOC are then introduced. These ideas can lead naturally to the power law scaling of the probability distributions and fractal spectra of the intermittent turbulence associated with the coherent structures. In Section III.1.5, we provide some convincing arguments for intermittency and FSOC in the magnetospheric plasma sheet. In Section III.1.6, the concept of invariant scaling, the dynamic renormalization-group, and topological phase transitions are discussed. These are then related to the multifractal scaling across various physical scales and the fluctuation-induced nonlinear instabilities that may lead to the

triggering of global magnetic field reconfigurations such as substorms. In Section III.1.7, simple phenomenological and analogous intermittency models are described. The summary and reference sections then follow.

III.1.2. Stochastically Distributed Coherent Structures in the Geospace Environment

In situ observations indicate that the dynamical processes in the geoplasma environment (e.g., the magnetotail region [Angelopoulos et al., 1996; Lui, 1996; 1998; Nagai et al., 1998]), generally entail localized intermittent processes and anomalous global transports. It was suggested by Chang [1998a,b,c; 1999] that instead of considering the turbulence as a mixture of interacting waves, such type of patchy intermittency could be more easily understood in terms of the development, interaction, merging, preferential acceleration and evolution of coherent magnetic structures.

Most field theoretical discussions begin with the concept of propagation of waves. For example, in the MHD formulation, one can combine the basic equations and express them in the following propagation forms:

$$\rho d\mathbf{V}/dt = \mathbf{B}\cdot\nabla\mathbf{B} + \cdots, d\mathbf{B}/dt = \mathbf{B}\cdot\nabla\mathbf{V} + \cdots \qquad (1)$$

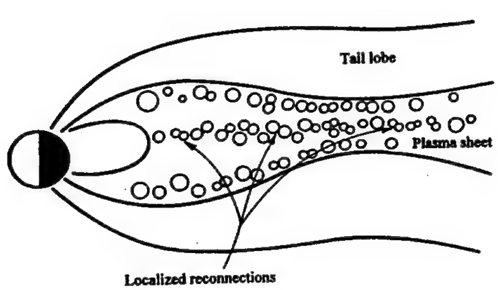

Figure 1. Cross-sectional view of flux tubes in the plasma sheet of the Earth's magnetotail

where the ellipsis represent the effects of the anisotropic pressure tensor, the compressible and dissipative effects, and all notations are standard. Equations (1) admit the well-known Alfvén waves. For such waves to propagate, the propagation vector $\mathbf{k}$ must contain a field-aligned component, i.e.,

$\mathbf{B}\cdot\nabla \rightarrow i\mathbf{k}\cdot\mathbf{B} \neq 0$. However, at sites where the parallel component of the propagation vector vanishes (the resonance sites), the fluctuations are localized. That is, around these resonance sites (usually in the form of curves), it may be shown that the fluctuations are held back by the background magnetic field, forming coherent magnetic structures in the form of flux tubes [Chang, 1998a,b,c; 1999]. For the neutral sheet region of the magnetotail, these structures are essentially current filaments in the cross-tail direction, Fig. 1. The results of a 2D MHD simulation showing such coherent structures are given in Fig. 2.

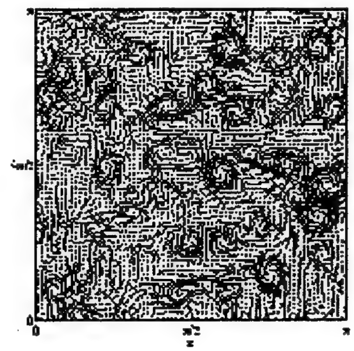

Figure 2. 2D simulation

Generally, there are various types of propagation modes (whistler modes, lower hybrid waves, etc.) in a geoplasma. Thus, we envision a corresponding number of different types of plasma resonances and associated coherent magnetic structures that typically characterize the dynamics of a plasma medium under the influence of a background magnetic field. These coherent structures will wiggle, migrate, deform and undergo different types of motions (including preferential acceleration), i.e., anisotropic stochastic randomization, under the influence of the local and global plasma and magnetic topology. It is this type of motion (evolution) and interaction of the coherent structures that characterize the dynamics of turbulent plasma, not plane waves.

III.1.3. Preferential Acceleration of BBF

Consider the coherent magnetic structures discussed in the previous section, which in the neutral sheet region of the plasma sheet are essentially filaments of concentrated currents in the cross-tail direction. We expect that, in a sheared magnetic

field that typically exists in the region under consideration, these multiscale fluctuations can supply the required coarse-graining dissipation that can produce nonlinear instabilities leading to "X-point-like" structures of the averaged magnetic field lines. For example, for a sheared magnetic field $B_x(z)$, upon the onset of such fluctuation-induced nonlinear instabilities, the averaged magnetic field will generally acquire a z-component. Let us choose x as the Earth-magnetotail direction (positive toward the Earth) and y in the cross-tail current direction. Then the deformed magnetic field geometry after the development of a mean field "X-point" magnetic structure will generally have a positive (negative) B_z component earthward (tailward) of the X-point. Near the neutral sheet region, the Lorentz force will therefore preferentially accelerate the coherent structures (which are essentially current filaments with polarities primarily pointing in the positive y-direction) earthward if they are situated earthward of the X-point and tailward if they are situated tailward of the X-point, Fig. 3. These results would therefore match the general directions of motion of the observed BBF in the magnetotail [Nagai et al, 1998].

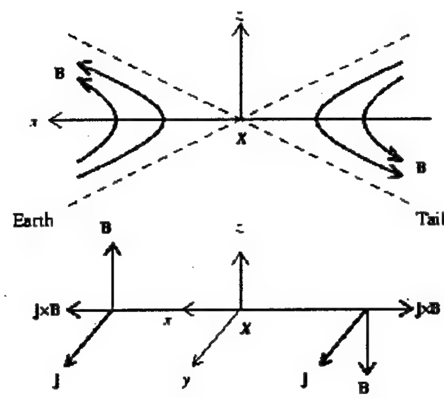

Figure 3. Schematic of a mean field X-point magnetic field geometry

We have performed preliminary two-dimensional numerical simulations to verify these conjectures. The simulations are based on a compressible MHD model that has been used by us in our previous studies of coherent magnetic structures [Wu and Chang, 2000a,b; 2001].

In the first example, we started the numerical simulation initially consisting of randomly distributed magnetic fluctuations. Eventually, after some elapsed time, multiscale coherent magnetic structures are formed, (Figure 4, left top panel; left panels are magnetic fields and right panels are flow vectors.). At this time, a uniform B_z is introduced. In the middle panels of Fig. 4, the effect of the Lorentz force is clearly seen through the motions of the coherent structures after some additional elapsed time. If the direction of B_z is reversed, the motions of the coherent structures are also reversed as seen in the bottom panels of Fig. 4.

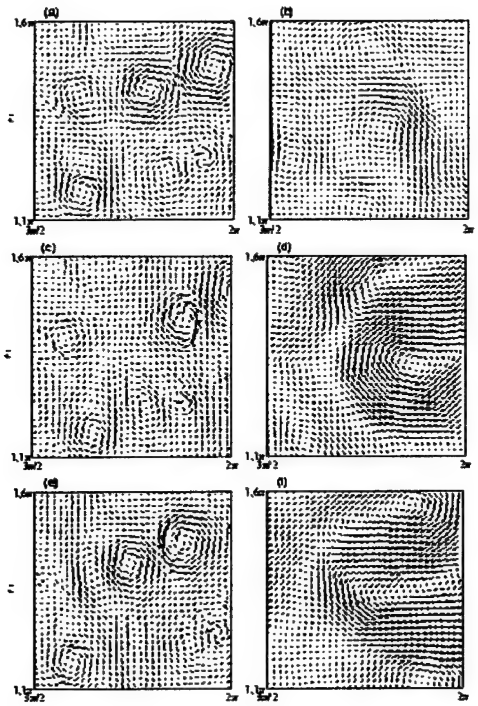

Figure 4. Effect of Lorentz force on the motion of the coherent structures

In the second example, we have considered the motions of the coherent magnetic structures that developed in a sheared magnetic field upon the initial introduction of random magnetic fluctuations. These structures were generally aligned in the x-direction near the neutral line, $z = 0$, after some elapsed time. A positive B_z was then applied. It can be seen (from Fig. 5; top panel: magnetic fields, bottom panel: flow vectors) that, after some additional elapsed time, the coherent structures (mostly oriented by currents in the positive y-direction), are generally accelerated in the positive

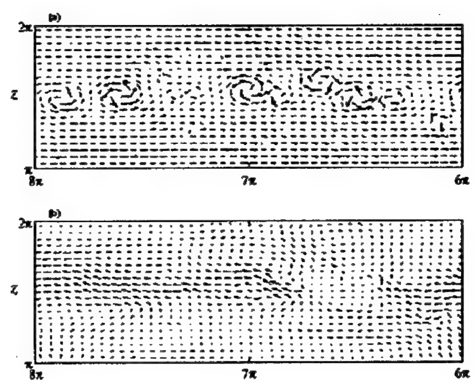

Figure 5. Effect of Lorentz force on coherent structures in a sheared field.

x-direction; with one exception where a pair of magnetic structures with oppositely directed currents effectively canceled out the net effect of the Lorentz force on these structures. We have plotted the x-component of the flow velocities v_x due to the cumulative effect of the Lorentz (and pressure) forces acting on the flow (and in particular the coherent structures) after some duration of time has elapsed (Fig. 6). We note that there are a number of peaks and valleys in the 3-dimensional display, with peak velocities nearly approaching that of the Alfvén speed mimicking the fast BBF that were observed in the magnetotail.. It is to be noted that an individual BBF event may be composed of one, two, or several coherent magnetic structures.

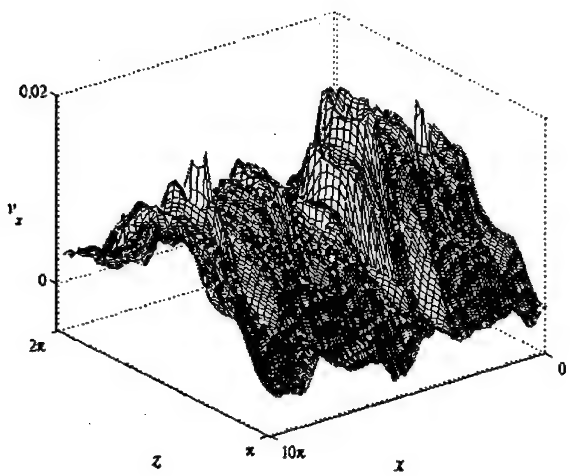

Figure 6. A 3D perspective of the v_x. The peak velocity of 0.02 is nearly the Alfvén velocity.

In Fig.7, we demonstrate in a self-consistent picture of what might occur near the neutral sheet region of the magnetotail. We injected randomly distributed magnetic fluctuations in a sheared magnetic field. The magnetic field geometry then underwent a fluctuation-induced nonlinear instability producing an X-point like mean field magnetic structure. The coherent

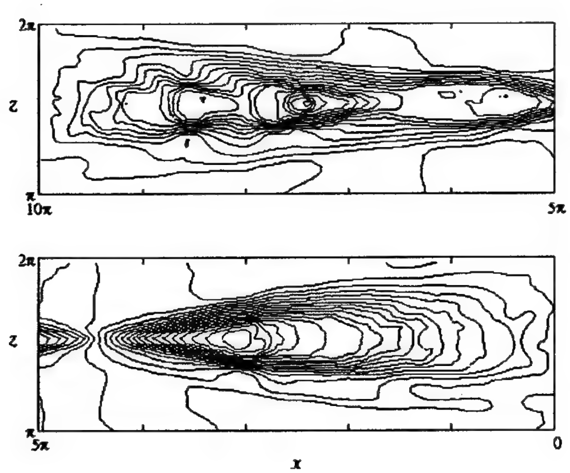

Figure 7. Contour plot of v_x in an X-point mean field magnetic geometry.

structures (aligned in the neutral sheet region) are subsequently accelerated by the induced B_z away from the X-point in both the positive and negative x-directions. Contour plots of v_x after some elapsed time clearly indicate such effects.

III.1.4. Localized Reconnections, FSOC and Power Law Scaling

As the coherent magnetic structures approach each other, randomly or due to external forcing, they may merge or scatter. Near the neutral sheet region, most of these structures carry currents of the same polarity (in the cross-tail direction). As two current filaments of the same polarity migrate toward each other, a strong current sheet is generated. The instabilities and turbulence generated by this strong current sheet can then initiate the merging of these structures. The results of such merging processes might be the origins of the signatures of localized reconnection processes detected by ISEE, AMPTE, and other spacecraft. The observed localized reconnection signatures to date seem to take place mainly in domain sizes comparable to that of the ion gyroradius. Thus, very probably, most of these processes are influenced by microscopic kinetic effects. During these dynamic processes, the ions can approximately be assumed to be unmagnetized and the electrons strongly magnetized, and the plasma nearly collisionless. This can lead to electron-induced Hall currents. With a general magnetic geometry, whistler fluctuations may usually be generated.

Now, in analogy to the Alfvénic resonances, singularities of $k_{\|} = \mathbf{k} \bullet \mathbf{B} = 0$ can develop at which whistler fluctuations cannot propagate. These "whistler resonances" can then provide the nuclear sites for the emergence of coherent whistler magnetic structures, which are the analog of the coherent Alfvénic magnetic structures but with much smaller scale sizes. The intermittent turbulence resulting from the intermixing and

interactions of the coherent whistler structures in the intense current sheet region can then provide the coarse-grain averaged dissipation that allows the filamentary current structures to merge, interact, or breakup. In addition to the above scenarios, other plasma instabilities may set in when conditions are favorable to initiate the merging and interactions.

FSOC. As the coherent magnetic structures merge and evolve, larger coherent structures are formed. At the same time, new fluctuations of various sizes are generated. These new fluctuations can provide the new nuclear sites for the emergence of new coherent magnetic structures. After some elapsed time, we expect the distributions of the sizes of the coherent structures to encompass nearly all observable scales. It has been argued by Chang [1992; 1998a,b,c; 1999] and briefly reviewed in Section 6 that, when conditions are favorable, a state of dynamic criticality (FSOC) might be approached. At such a state, the structures take on all scale sizes with a power-law probability distribution of the scale sizes of the fluctuations, as well as power-law frequency (ω) and mode number (k) spectra of the correlations of the associated fluctuations. Analyses of existing observations in the intermittent turbulence region of the magnetotail and those conjectured from the AE index seem to confirm such predictions [Consolini, 1997; Lui, 1998; Angelopoulos et al., 1999; Lui et al., 2000; Uritsky et al., 2002b]. In addition, these multiscale coherent structures may render the coarse-grained dissipation that sometimes provides the seeds for the excitation of nonlinear instabilities leading to, for example, the onset of substorms in the Earth's magnetosphere.

III.1.5. Observational Evidences for FSOC and Intermittency in Geospace Plasmas

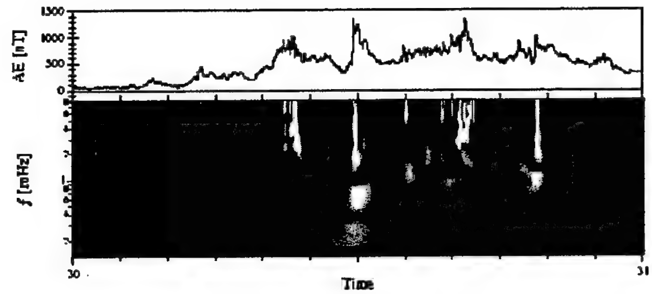

Figure 8. AE index behavior and the LIM measure.

The first definitive observation that provided convincing evidence indicating certain turbulent space plasma processes are in states of forced and/or self-organized criticality (FSOC) was the discovery of the apparent power-law probability distribution of solar flare intensities [Lu, 1995]. Recent statistical studies of complexity in geospace plasmas came from the AE index, UVI auroral imagery, and in-situ measurements related to the dynamics of the plasma sheet in the Earth's magnetotail. For example, the power-law spectra of AE burst occurrences as a function of AE burst strength has provided an important indication that the magnetosphere system is generally in a state of FSOC [Consolini, 1997]. More recent evaluations of the local intermittency measure (LIM) using the Morlett wavelet (Figure 8, from Consolini and Chang [2001]) clearly identified the burst contributions to the AE index. These results strongly suggest that the Earth's plasma sheet, particularly during substorms times, are bursty and intermittent. Some of the salient features of the complexity studies using the UVI imagery and in-situ flow measurements in the plasma sheet region verifying these suggestions are briefly described below.

(i) Auroral UVI Images

UVI images provide detailed information on the dynamics of spatially distributed magnetotail activity covering extended observation periods. It has been shown that the positions of auroral active regions in the nighttime magnetosphere are correlated with the position of the plasma sheet instabilities [Fairfield et al., 1999; Lyons et al., 1999; Sergeev et al., 1999; Ieda et al., 2001; Nakamura et al., 2001a; 2001b], whereas timing of the auroral disturbances provides good estimates for both small-scale isolated plasmoid releases [Ieda et al., 2001] and for the global-scale substorm onset times [Germany et al., 1998; Newell et al., 2001].

Recently, Lui et al. [2000] used global auroral UVI imagery from the POLAR satellite to obtain the statistics of size and energy dissipated by the magnetospheric system as represented by the intensity of auroral emission on a worldwide scale. They found that the internal relaxations of the magnetosphere statistically follow power laws that have the same index independent of the overall level of activity. The analysis revealed two types of energy dissipation: those internal to the magnetosphere occurring at all activity levels with no intrinsic scale, and those associated with active times corresponding to global energy dissipation with a characteristic scale.

Uritsky et al. [2002b] have performed an extensive analysis of the probability distributions of spatiotemporal magnetospheric disturbances as seen in POLAR UVI images of the nighttime ionosphere.

They observed power-law statistics for the probability distributions of the integrated sizes and energies, that are consistent with the behavior of numerical models operating near the FSOC point; they provide important observational evidence for

stationary critical dynamics in the magnetosphere. Based on this result, one can expect cross-scale coupling effects to play a significant, if not crucial, role in the development of geomagnetic disturbances. More specifically, the FSOC principle implies that large-scale properties of the magnetotail plasma sheet depend critically on the statistical hierarchy of small- and intermediate-scale perturbations associated with sporadic magnetic reconnections, current sheet disruptions, and other localized plasma instabilities [Klimas et al., 2000a,b].

(ii) Evidence of Intermittency and Power-Law Behavior of Bursty Bulk Flow (BBF) Durations in Earth's Plasma Sheet

Statistical analyses based on in-situ data collected by the GEOTAIL satellite have yielded convincing proof of intermittent turbulence with power law correlations [Angelopoulos et al., 1999]. It was shown that the magnetotail is generally in a bi-modal state: nearly stagnant, except when driven turbulent by transport efficient fast flows. Figure 9 displays the probability density functions of the *X*-component of the plasma

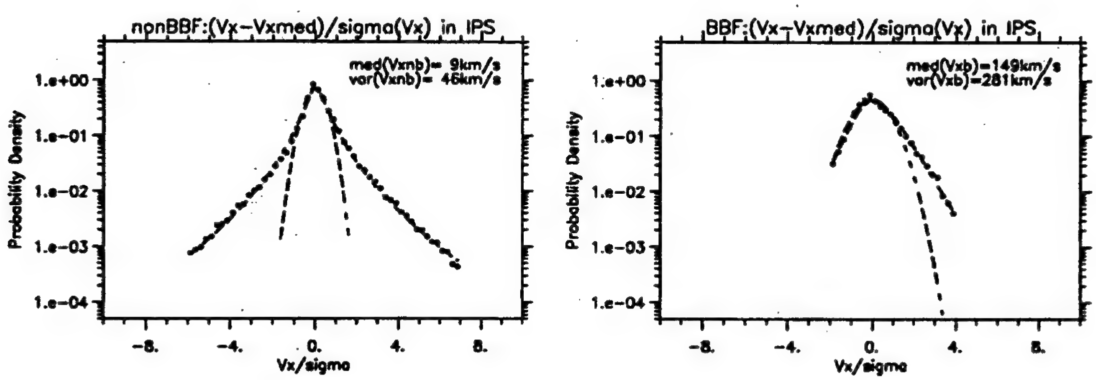

Figure 9. Probability distributions of the non-BBF and BBF x-component of the normalized flows along with best fits of Gaussian and Castaing functions.

sheet flows for both the bursty bulk flow (BBF) and non-BBF populations. Both distributions are clearly non-Gaussian and both can be fitted nicely with the Castaing et

al. [1990] distributions indicating intermittency for both components of flow in the plasma sheet.

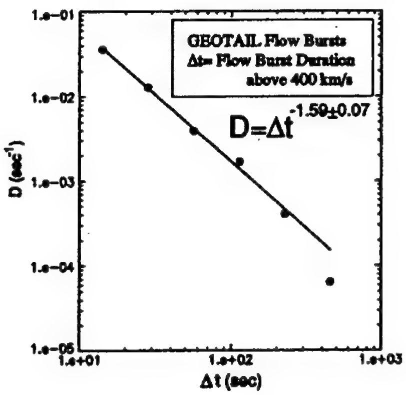

Figure 10. Probability density of BBF bursts in the plasma sheet.

Figure 10 shows the probability density function of the flow magnitude durations above 400 km/s in the inner plasma sheet [Angelopoulos et al., 1999]. The plasma sheet was selected on the basis of plasma pressure ($P_i > 0.01 nPa$) but very similar results are obtained by confining the data in the near-neutral sheet region using plasma beta ($\beta_i > 0.5$). A power law is clearly indicated. The power-law behavior with spectral index ~-1.6 remains when the velocity magnitude threshold is changed to a lower or higher value, and when different spatial regions of the magnetotail plasma sheet in the *X*-*Y* plane are considered, indicating that the results are quite robust. The results for linear binning in flow duration, Δt, are identical to the ones from logarithmic binning presented in the figure. Thus, there is strong indication that the energy dissipation in the magnetotail adheres to the behavior expected from FSOC.

III.1.6. Invariant Scaling and Topological Phase Transitions.

In the previous section, we mentioned the possibility of the existence of "complex" topological states that can exhibit the characteristic phenomenon of dynamic criticality similar to that of equilibrium phase transitions. By "complex" topological states we mean magnetic topologies that are not immediately deducible from the elemental (e.g., MHD and/or Vlasov) equations [Consolini and Chang, 2001]. Below, we shall briefly address the salient features of the analogy between topological and

equilibrium phase transitions. A thorough discussion of these ideas may be found in Chang [1992, 1999; 2001, and references contained therein.]

For nonlinear stochastic systems near criticality, the correlations among the fluctuations of the random dynamical fields are extremely long-ranged and there exist many correlation scales. The dynamics of such systems are notoriously difficult to handle either analytically or numerically. On the other hand, since the correlations are extremely long-ranged, it is reasonable to expect that the system will exhibit some sort of invariance under scale transformations. A powerful technique that utilizes this invariance property is the technique of the dynamic renormalization-group [Chang et al., 1978; 1992; and references contained therein]. As it is described in these references, based on the path integral formalism, the behavior of a nonlinear stochastic system far from equilibrium may be described in terms of a "stochastic Lagrangian L". Then, the renormalization-group (coarse-graining) transformation may be formally expressed as:

$$\partial L / \partial \ell = RL \tag{2}$$

where R is the renormalization-group (coarse-graining) transformation operator and ℓ *is* the coarse-graining parameter for the continuous group of transformation. It will be convenient to consider the state of the stochastic Lagrangian in terms of its parameters $\{P_n\}$. Equation (2), then, specifies how the Lagrangian, L, flows (changes) with ℓ in the affine space spanned by $\{P_n\}$, Fig. 11.

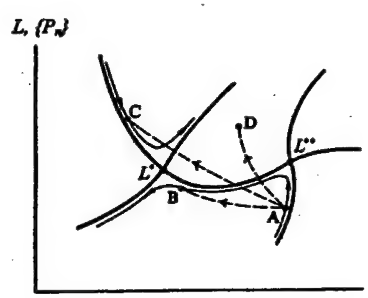

Figure 11. Renormalization-group trajectories and fixed points.

Generally, there exists a number of fixed points (singular points) in the flow field, where $dL/d\ell = 0$. At a fixed point (L^* or L^{**} in Fig.11), the correlation length should not be

changing. However, the renormalization-group transformation requires that all length scales must change under the coarse-graining procedure. Therefore, to satisfy both requirements, the correlation length must be either infinite or zero. When it is at infinity, the system is by definition at criticality. The alternative trivial case of zero correlation length will not be considered here.

To study the stochastic behavior of a nonlinear dynamical system near a particular criticality (e.g., the one characterized by the fixed point L^*), we can linearize the renormalization-group operator R about L^*. The mathematical consequence of this approximation is that, close to criticality, certain linear combinations of the parameters that characterize the stochastic Lagrangian L will correlate with each other in the form of power laws. This includes, in particular, the (k, ω), i.e. mode number and frequency, spectra of the correlations of the various fluctuations of the dynamic field variables. In addition, it can be demonstrated from such a linearized analysis that generally only a small number of (relevant) parameters are needed to characterize the stochastic state of the system near criticality [i.e., low-dimensional behavior; see Chang (1992)].

Symmetry Breaking and Topological Phase Transitions. As the dynamical system evolves in time (autonomously or under external forcing), the state of the system (i.e., the values of the set of the parameters characterizing the stochastic Lagrangian, L) changes accordingly. A number of dynamical scenarios are possible. For example, the system may evolve from a critical state A (characterized by L^{**}) to another critical state B (characterized by L^*) as shown in Fig. 11. In this case, the system may evolve continuously from one critical state to another. On the other hand, the evolution from the critical state A to critical state C as shown in Fig. 11 would probably involve a dynamical

instability characterized by a first-order-like topological phase transition because the dynamical path of evolution of the stochastic system would have to cross over a couple of topological (renormalization-group) separatrices. Alternatively, a dynamical system may evolve from a critical state A to a state D (as shown in Fig. 11) which may not be situated in a regime dominated by any of the fixed points; in such a case, the final state of the system will no longer exhibit any of the characteristic properties that are associated with dynamic criticality. Alternatively, the dynamical system may deviate only moderately from the domain of a critical state characterized by a particular fixed point such that the system may still display low-dimensional scaling laws, but the scaling laws may now be deduced from straightforward dimensional arguments. The system is then in a so-called mean-field state. (For general references of symmetry breaking and nonlinear crossover, see Chang and Stanley [1973]; Chang et al., [1973a; 1973b]; Nicoll et al., [1974; 1976]).

III.1.7. Modeling of Dynamic Intermittency

(i) Triggered Local Order-Disorder Transitions.

As noted in the previous section, the "complex" behavior associated with the intermittent turbulence in magnetized plasmas may generally be traced directly to the sporadic and localized interactions of magnetic coherent structures. Coherent structures may merge and form more energetically favorable configurations. They may also become unstable (either linearly or nonlinearly) and bifurcate into smaller structures. The origins of these interactions may arise from the effects of the various MHD and kinetic (linear and nonlinear) instabilities and the resultant finer-scale turbulences.

Such localized sporadic interactions may be modeled by the triggered (fast) localized chaotic growth of a set of relevant order parameters, $O_i (i = 1, 2, N)$:

$$\partial O_i / \partial t = \psi_i(\mathbf{O},\mathbf{P};c_1,c_2 \cdots c_n;\tau_1,\tau_2 \cdots \tau_n), \tag{3}$$

where "ψ_i" are functionals of $(\mathbf{O},\mathbf{P})$, $\mathbf{P}(\mathbf{x},t) = P_j(j=1,2,...M)$ are the state variables (or control parameters), $(\mathbf{x},t)$ are the spatial and temporal variables, the c_n's are a set of triggering parameters and the τ's are the corresponding relaxation time scales characterizing the localized intermittencies, which, in general, are much smaller than those characterizing the evolutionary time scales for the state variables.

For the special case of a single one-dimensional order parameter O, let us assume that the driving term may be expressed in terms of a real-valued state function (the local configurational free energy), $F(O,\mathbf{P};c_1,c_2 \cdots c_n;\tau_1,\tau_2 \cdots \tau_n)$, such that

$$\partial O / \partial t = -\partial F(O) / \partial O. \tag{4}$$

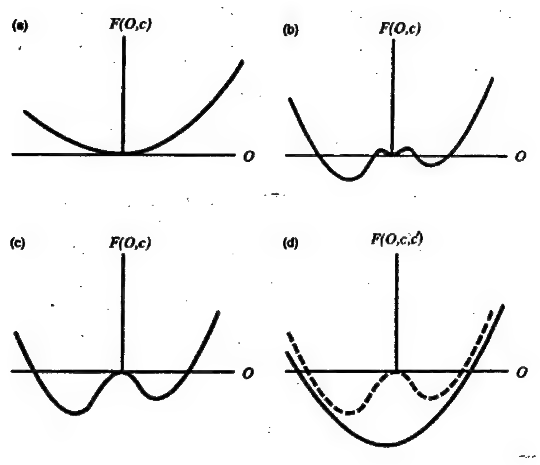

Figure 12. Topologies of state function $F(O)$.

Generally, the topology of the value of the state function F will contain valleys and hills in the real space spanned by the order parameters O at each given (x,t). If F is real, continuous with continuous derivatives, then we may visualize F locally in terms of a real polynomial function of O. The topology of the state function $F(O)$ may take on forms that are (1) locally stable, Figure 12a, (2) locally nonlinearly unstable, Figure 12b, and (3) locally linearly unstable (bifurcation), Figure 12c. States (2) and (3) may be triggered by a critical parameter $c > 0$ (with a corresponding relaxation time scale τ with or without nonlinear fluctuations. For the triggering of a locally nonlinear instability, the triggering

parameter would typically be some sort of a measure of the amplitude of the local nonlinear fluctuations. For the triggering of a local linear instability, the triggering parameter would generally be some sort of a measure of the amplitude of the local gradient of the state variable, P. (We note that a similar but symmetrical model based on the Landau-Ginsburg expansion has been considered by Gil and Sornette [1996]).

Alternatively, a locally bifurcated state such as state (3) may be influenced by another triggering parameter $c'>0$ such that a more preferred local state similar to that of state (1) becomes energetically more favorable than that of the bifurcated state. See Figure 12d.

One may easily connect such local triggering behavior of order-disorder transitions to those of the localized, sporadic interactions of the magnetic coherent structures discussed in the previous section. For example, the situation depicted by Figure 12d can be interpreted as the merging of two coherent structures. Also, states (2) and (3) can be interpreted as the bifurcation of one coherent structure into two smaller coherent structures due to certain nonlinear or linear plasma instability. Because most of such processes are probably due to the result of certain kinetic effects, the interaction time-scales would generally be of the order of kinetic reaction-times and therefore much shorter then the system evolution-time to be described in the following section.

(ii) Transport Equations of State Variables

The (slow time) evolution equations of the state variables will generally consist of convective, forcing, random stirring, and transport terms. Typically, they may take on the following generic form:

$$\partial P_j / \partial t = \zeta_j(\mathbf{P},\mathbf{O};\upsilon_1,\upsilon_2,\cdots\upsilon_m) \qquad (5)$$

where $\zeta_j (j=1,2,\cdots M)$ are functionals of $(\mathbf{P},\mathbf{O})$ and the υ's are a set of time scales characterizing the long time system-wise evolution under the influence of the chaotic and anomalous growths of the triggered order parameters.

For a one-dimensional single real-valued state variable, one might envisage the following typical transport equation in differential form:

$$\partial P/\partial t = f + h(P,O)\partial P/\partial x + D\partial^2 P/\partial x^2 + g \tag{6}$$

where f is the forcing term, $h(P,O)$ is a convective function, g is a random noise, and $D = D_0 H(O)$ is the anomalous transport coefficient with $H(O)$, a positive-definitive growing function of the magnitude of the absolute value of O.

From this example (as well as the general expression, (5)), we note that the anomalous transport and convection can take on varying magnitudes (because of their dependence on the order parameter) and it is generally sporadic and localized throughout the system. Such behavior naturally leads to the evolution of fluctuations into all spatial and temporal scales, and would generally lead the global system to evolve into a "complex" state of long-range interactions exhibiting the phenomenon of forced and/or self-organized criticality (FSOC) as has been discussed extensively in several of our previous publications [Chang, 1998a,b,c; 1999; 2001; Wu and Chang, 2000a,b; 2001].

(iii) An Illustrative Example.

We consider below a simple 2-D phenomenological model to mimic non-resonant MHD turbulence. We introduce the flux function ψ for the non-resonant transverse fluctuations such that $(-\partial\psi/\partial x, \partial\psi/\partial y) = (\delta B_y, \delta B_x)$ and $\nabla\bullet\delta\mathbf{B} = 0$. The coherent structures for such a system are generally flux tubes normal to the 2-D plane such as those simulated in Fig. 2. Instead of invoking the standard 2-D MHD formalism, here we

simply consider ψ as a dynamic order parameter. As the flux tubes merge and interact, they may correlate over long distances, which, in turn, will induce long relaxation times near FSOC. Assuming homogeneity, we model the dynamics of flux tubes, in the crudest approximation, in terms of a classical Time-Dependent Landau-Ginsburg model as follows:

$$\partial \psi_k / \partial t = -\Gamma_k \partial F / \partial \psi_{-k} + f_k \tag{7}$$

where ψ_k are the Fourier components of the flux function, Γ_k an analytic function of k^2, and f_k a random noise which includes all the other effects that had been neglected in this crude model. We shall assume the state function to depend on the flux function ψ and the local energy measure ξ. For non-resonant fluctuations, we shall assume that diffusion dominates over convection. Thus, in addition to the dynamic equation (7), we now include a diffusion equation for ξ. In Fourier space, we have

$$\partial \xi_k / \partial t = -Dk^2 \partial F / \partial \xi_{-k} + h_k \tag{8}$$

where ξ_k are the Fourier components of ξ, $D(k)$ is the diffusion coefficient, $F(\psi_k, \xi_k, k)$ is the state function, and h_k is a random noise. By doing so, we separate the slow energy transport due to diffusion of the local energy measure ξ from the noise term f_k.

Under the dynamic renormalization group (DRG) transformation, the average of the square of the fluctuations of the flux function in Fourier space, C, should scale as:

$$e^{a_c \ell} C(k, \omega) = C(k e^{\ell}, \omega e^{a_\omega \ell}) \tag{9}$$

where ω is the Fourier transform of the time t, ℓ the renormalization parameter as defined in the previous section, and (a_c, a_ω) the correlation and dynamic exponents.

Thus, $C/\omega^{a_c/a_\omega}$ is an absolute invariant under the DRG, or $C \sim \omega^{-\lambda}$, where $\lambda = -a_c/a_\omega$. DRG analyses performed for Gaussian noises for several approximations yield the value for λ to be approximately equal to 1.88 - 1.66, and a value of -1.0 for the ω-exponent for the trace of the transverse magnetic correlation tensor. Interestingly, Matthaeus and Goldstein [1986] had suggested that such a magnetic correlation exponent might represent the dynamics of discrete structures in pseudo 2-D non-resonant turbulence; thus, giving some credence to the model and the DRG analysis.

(iv) An Analogous Example--the Global Modified Forest-Fire Model

While it will be the main goal of this proposed research to develop physically realistic models to study the "complexity" of the magnetotail, we demonstrate in this section an analogous model, which seems to encompass some of the basic characteristics of what are expected for the dynamical magnetotail.

We describe below the global generalization [Tam et al., 2000b] of a "modified forest-fire model" originally introduced by Bak et al. [1990] and modified by Drossel and Schwabl [1992]. Let us consider a rectangular grid of land, on which trees may grow at any given site (i, j) and any time step n with a probability p. At sites where there is a tree, there is a finite probability f that it might be hit by lightning and catch fire. If a tree catches fire at certain time step n, then its neighbor will catch fire at a subsequent time step $n+1$. It is obvious that at any given time step n, there will be patches of green trees, patches of burning trees and patches of empty spaces, Fig. 13 (courtesy of G. Consolini). One may associate the growth of trees as the development of coherent structures, the burning trees as localized merging sites and empty spaces as quiescent

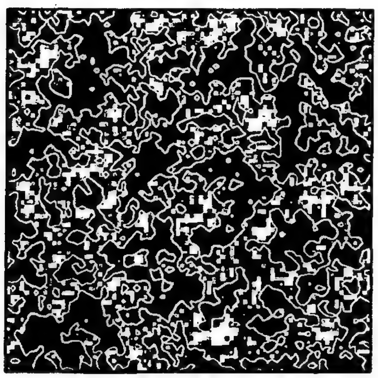

Figure 13. Snapshot of forest-fire simulation.

states in the magnetotail, a picture simulating the sporadically growing of coherent magnetic structures with localized merging.

The incremental changes of the probabilities (p, f), and the densities of the green trees, burning trees and empty spaces (ρ_1, ρ_2, ρ_3), characterize the dynamics of the forest fire. In particular, (p, f) are the dynamic parameters, and the densities are the dynamic state variables. Following the discussions given in the previous section, we perform a renormalization (coarse-graining) transformation of the parameters (p, f) such that the phenomenon retains its essential basic characteristics. Let us symbolically denote this transformation as:

$$p' = F(p, f; \rho_1, \rho_2, \rho_3); \qquad f' = G(f, p; \rho_1, \rho_2, \rho_3) \tag{10}$$

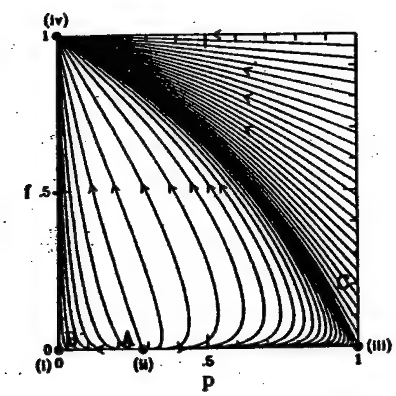

Figure 14. Renormalization group trajectories.

When the system reaches a steady state, the densities, (ρ_1, ρ_2, ρ_3), may be obtained from the mean field theory at any level of coarse-graining and are expressible in terms of the dynamic parameters (p, f).

In Figure 14, we show the affine space of transformations of (p, f) for a particular choice of renormalization group procedure [Tam et al., 2000b] (a global generalization of the coarse-graining procedure suggested by Loreto et al. [1995]) in the physically meaningful region of (p, f) between (0, 1). We note that there are 4 distinct fixed points. Each fixed point has its own distinct dynamic critical behavior. In

the figure, the renormalization trajectories are displayed as solid curves with arrows indicating the direction of coarse-graining. If the dynamic state of the forest-fire is at a state A near the fixed point (ii), then the system will exhibit the characteristic critical behavior prescribed by the invariance properties of this fixed point until sufficient coarse-graining has taken place such that the renormalized system approaches a point such as B in a region dominated by the fixed point (i). At this point, in the coarse-grained view, the dynamical system will now exhibit the critical behavior characterized by the fixed point (i). We have calculated this crossover (symmetry breaking) behavior for the power-law index of the probability distribution $P(s)$ of the scale sizes of the burnt trees, Figure 15. In terms of the magnetotail analogy, such type of crossover behavior might be associated with the change of physical behavior from the kinetic state to the MHD state. We note that there is a distinct separatrix connecting the fixed points (iii) and (iv). Thus, transition from a dynamic state such as B to a dynamic state such as C generally cannot be smooth and is probably catastrophic. This would be the analog of the triggering of the onset of substorms due to coarse-grained dissipation in the magnetotail. Although not detailed here, there are many other properties of this analogous model that resemble the magneotail dynamics.

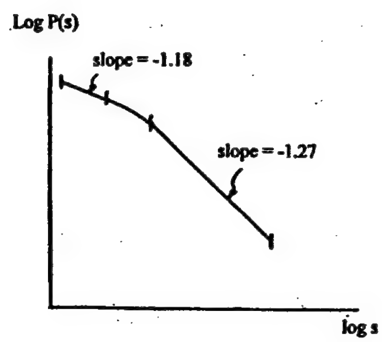

Figure 15. Crossover between two fixed points.

III.1.8. Summary

We have presented a dynamical theory of "complexity" for space plasmas far from equilibrium. The theory is based on the physical concepts of mutual interactions of coherent magnetic structures that emerge naturally from plasma resonances.

Models are constructed to represent the local intermittencies and global evolutional processes. Dynamical renormalization-group techniques are introduced to handle the stochastic nature of the model equations that exhibit "complexity". Examples are provided to illustrate the phenomena of anomalous transports, preferential acceleration, forced and/or self-organized criticality [FSOC], symmetry breaking and general topological phase transitions including the reconfigurations of mean magnetic field geometries due to coarse-grained dissipation.

Both the physical concepts and mathematical techniques are nontraditional. The readers are encouraged to consult the original references for further in-depth studies of these new emerging ideas.

III.1. 9. References

Angelopoulos, V., F.V. Coroniti, C.F. Kennel, M.G. Kivelson, R.J. Walker, C.T. Russell, R.L. McPherron, E. Sanchez, C.I. Meng, W. Baumjohann, G.D. Reeves, R.D. Belian, N. Sato, E. Fris-Christensen, P.R. Sutcliffe, K. Yumoto and T. Harris, Multi-point analysis of a BBF event on April 11, 1985, *J. Geophys. Res.,* 101, 4967, 1996.

Angelopoulos, V., T. Mukai and S. Kokubun, Evidence for intermittency in Earth's plasma sheet and implications for self-organized criticality, *Physics of Plasmas*, 6, 4161, 1999.

Bak, P., K. Chen, and C. Tang, A forest-fire model and some thoughts on turbulence, *Physics Letters*, A147, 297, 1990.

Castaing, B., Y. Gagne, and E.J. Hopfinger, Velocity probability density functions of high Reynolds number turbulence, *Physica D*, 46, 177, 1990.

Chang, T., and H.E. Stanley, Renormalization-group verification of crossover with respect to lattice anisotropy parameter, *Phys. Rev.*, B8, 1178, 1973.

Chang, T., A. Hankey, and H.E. Stanley, Double-power scaling functions near tricritical points, *Phys. Rev.*, B7, 4263, 1973a.

Chang, T., A. Hankey, and H.E. Stanley, Generalized scaling hypothesis in multi-component systems. I. Classification of critical points by order and scaling at tricritical points, *Phys. Rev.*, B8, 346, 1973b.

Chang, T., J.F. Nicoll and J.E. Young, A closed-form differential renormalization-group generator for critical dynamics, *Physics Letters*, 67A, 287, 1978.

Chang, T., Low-dimensional behavior and symmetry breaking of stochastic systems near criticality - can these effects be observed in space and in the laboratory?, *IEEE Trans. on Plasma Science*, 20, 691, 1992.

Chang, T., D.D. Vvedensky and J.F. Nicoll, Differential renormalization-group generators for static and dynamic critical phenomena, *Physics Reports*, 217, 279, 1992.

Chang, T., Sporadic, localized reconnections and multiscale intermittent turbulence in the magnetotail, *AGU Monograph on "Geospace Mass and Energy Flow"*, ed. Horwitz, J.L., D.L. Gallagher, and W.K. Peterson, Am. Geophys. Union, Washington, D.C., v. 104, p. 193, 1998a.

Chang, T., Multiscale intermittent turbulence in the magnetotail, *Proc. 4th Intern. Conf. on Substorms*, ed. Kamide, Y. et al., Kluwer Academic Publishers, Dordrecht and Terra Scientific Publishing Company, Tokyo, p. 431, 1998b.

Chang, T., Self-organized criticality, multi-fractal spectra, and intermittent merging of coherent structures in the magnetotail, *Astrophysics and Space Science,* ed. Büchner, J., et al., Kluwer Academic Publishers, Dordrecht, Netherlands, v. 264, p. 303, 1998c.

Chang, T., Self-organized criticality, multi-fractal spectra, sporadic localized reconnections and intermittent turbulence in the magnetotail, *Physics of Plasmas*, 6, 4137, 1999.

Chang, T., Colloid-like behavior and topological phase transitions in space plasmas: intermittent low frequency turbulence in the auroral zone, *Physica Scripta,* T89, 80, 2001.

Chapman, S.C., N.W. Watkins, R.G. Dendy, P. Helander and G. Rowlands, A simple avalanche model as an analogue for magnetospheric activity, *Geophys. Res. Lett.,* 25, 2397, 1998.

Consolini, G., M.F. Marcucci, and H. Candidi, Multifractal structure of auroral electrojet index data, *Phys. Rev. Lett.*, *76* (21), 4082-4085, 1996.

Consolini, G., Sandpile cellular automata and magnetospheric dynamics, in *Cosmic Physics in the Year 2000,* edited by S. Aiello, N. Lucci, G. Sironi, A. Treves, and U. Villante, pp. 123-126, Soc. Ital. di Fis., Bologna, Italy, 1997.

Consolini, G., and M.F. Marcucci, Multifractal structure and intermittence in the AE index time series, *Nuovo Cimento Della Societa Italiana Di Fisica C-Geophysics and Space Physics*, *20* (6), 939-949, 1997.

Consolini, G., and T. Chang, "Magnetic Field Topology and Criticality in Geotail Dynamics: Relevance to Substorm Phenomena", *Space Science Reviews*, 95, 309, 2001.

Drossel, B., and F. Schwabl, Self-organized critical forest-fire model, *Phys. Rev. Lett.*, 69, 1629, 1992.

Fairfield, D.H., T. Mukai, M. Brittnacher, G.D. Reeves, S. Kokubun, G.K. Parks, T. Nagai, H. Matsumoto, K. Hashimoto, D.A. Gurnett, and T. Yamamoto, Earthward flow bursts in the inner magnetotail and their relation to auroral brightenings, AKR intensifications, geosynchronous particle injections and magnetic activity, *J. Geophys. Res.*, *104* (A1), 355-370, 1999.

Germany, G.A., G.K. Parks, H. Ranganath, R. Elsen, P.G. Richards, W. Swift, J.F. Spann, and M. Brittnacher, Analysis of auroral morphology: Substorm precursor and onset on January 10, 1997, *Geophys. Res. Lett.*, *25* (15), 3043-3046, 1998.

Gil, L., and D. Sornette, Laudau-Ginzburg theory of self-organized criticality, *Phys. Rev. Lett.*, 76, 3991, 1996.

Gleisner, H., and H. Lundstedt, A neural network-based local model for prediction of geomagnetic disturbances, *J. Geophys. Res.*, *106* (A5), 8425-8433, 2001.

Horton, W., and I. Doxas, A low-dimension energy-conserving state space model for substorm dynamics, *J. Geophys. Res.*, *101* (A12), 27223-27237, 1996.

Horton, W., and I. Doxas, A low-dimensional dynamical model for the solar wind driven geotail-ionosphere system, *J. Geophys. Res.*, *103* (A3), 4561-4572, 1998.

Hosino, M., A. Nishida and T. Yamamoto, Turbulent magnetic field in the distant magnetotail: Bottom-up process of plasmoid formation, *Geophys. Res. Lett.,* 21, 2935, 1994.

Ieda, A., D.H. Fairfield, T. Mukai, Y. Saito, S. Kokubun, K. Liou, C.-I. Meng, G.K. Parks, and M.J. Brittnacher, Plasmoid ejection and auroral brightenings, *Journal of Geophysical Research - Space Physics*, *106* (A3), 3845-3857, 2001.

Jiang, G.S., and C.C. Wu, A high order finite difference scheme for the equations of ideal magnetohydrodynamics, *J. Comp. Phys.,* 150, 549, 1999.

Kinouchi, O., and C.P.C. Prado, Robustness of scale invariance in models with self-organized criticality, *Phys. Rev. E*, *59* (5), 4964-4969, 1999.

Klimas, A.J., D.N. Baker, D.A. Roberts, D.H. Fairfield, and J. Buchner, A nonlinear dynamic analog model of geomagnetic activity, *J. Geophys. Res.*, *97* (A8), 12,253-12,266, 1992.

Klimas, A.J., D.N. Baker, D. Vassiliadis, and D.A. Roberts, Substorm recurrence during steady and variable solar wind driving: Evidence for a normal mode in the unloading dynamics of the magnetosphere, *J. Geophys. Res.*, *99* (A8), 14,855-14,861, 1994.

Klimas, A.J., D. Vassiliadis, D.N. Baker, and D.A. Roberts, The organized nonlinear dynamics of the magnetosphere, *J. Geophys. Res.*, *101* (A6), 13,089-13,113, 1996.

Klimas, A.J., D. Vassiliadis, and D.N. Baker, Data-derived analogues of the magnetospheric dynamics, *J. Geophys. Res.*, *102* (A12), 26,993-27,009, 1997.

Klimas, A.J., V. Uritsky, J.A. Valdivia, D. Vassiliadis, and D.N. Baker, On the compatibility of the coherent substorm cycle with the complex plasma sheet, in *International Conference on Substorms-5*, edited by O. Troshichev, and V. Sergeev, pp. 165-168, ESA Publications Division, St. Petersburg, Russia, 2000a.

Klimas, A.J., J.A. Valdivia, D. Vassiliadis, D.N. Baker, M. Hesse, and J. Takalo, Self-organized criticality in the substorm phenomenon and its relation to localized reconnection in the magnetospheric plasma sheet, *J. Geophys. Res.*, *105* (A8), 18,765-18,780, 2000b.

Kurganov, A., and E. Tadmor, New high-resolution central schemes for nonlinear conservation laws and convection-diffusion equations, *J. Comp. Phys.*, 160, 214, 2000.

Loreto, V., L. Pietronero, A. Vespignani, and S. Zapperi, Renormalization group approach to the critical behavior of the Forest-Fire model, *Phys. Rev. Lett.*, 75, 465, 1995.

Lui, A.T.Y., Current disruptions in the Earth's magnetosphere: observations and models, *J. Geophys. Res.*, 101, 4899, 1996.

Lui, A.T.Y., Plasma sheet behavior associated with auroral breakups, *Proc. 4th Intern. Conf. on Substorms,* ed. Y. Kamide, Kluwer Academic Publishers, Dordrecht and Terra Scientific Publishing Company, Tokyo, p. 183, 1998.

Lui, A.T.Y., S.C. Chapman, K. Liou, P.T. Newell, C.I. Meng, M. Brittnacher, and G.D. Parks, Is the dynamic magnetosphere an avalanching system?, *Geophys. Res. Lett.*, *27* (7), 911-914, 2000.

Lyons, L.R., T. Nagai, G.T. Blanchard, J.C. Samson, T. Yamamoto, T. Mukai, A. Nishida, and S. Kokubun, Association between Geotail plasma flows and auroral poleward boundary intensifications observed by CANOPUS photometers, *J. Geophys. Res.*, *104* (A3), 4485-4500, 1999.

Matthaeus, W.H., and M.L. Goldstein, Low-frequency 1/*f* noise in the interplanetary magnetic field, *Phys. Rev. Lett.*, 57, 495, 1986.

Milovanov, A., L. Zelenyi and G. Zimbardo, Fractal structures and power law spectra in the distant Earth's magnetotail, *J. Geophys. Res.,* 101, 19903, 1996.

Nagai, T., M. Fujimoto, Y. Saito, S. Machida, et al., Structure and dynamics of magnetic reconnection for substorm onsets with Geotail observations, *J. Geophys. Res.*, 103, 4419, 1998.

Nakamura, R., W. Baumjohann, M. Brittnacher, V.A. Sergeev, M. Kubyshkina, T. Mukai, and K. Liou, Flow bursts and auroral activations: Onset timing and foot point location, *J. Geophys. Res.*, *106* (A6), 10777-10789, 2001a.

Nakamura, R., W. Baumjohann, R. Schodel, M. Brittnacher, V.A. Sergeev, M. Kubyshkina, T. Mukai, and K. Liou, Earthward flow bursts, auroral streamers, and small expansions, *J. Geophys. Res.*, *106* (A6), 10791-10802, 2001b.

Nessyahu H., and E. Tadmor, Non-oscillatory central differencing for hyperbolic conservation laws, *J. Comp. Phys.,* 87, 408. 1990.

Newell, P.T., K. Liou, T. Sotirelis, and C.I. Meng, Polar Ultraviolet Imager observations of global auroral power as a function of polar cap size and magnetotail stretching, *J. Geophys. Res.*, *106* (A4), 5895-5905, 2001.

Nicoll, J.F., T. Chang, and H.E. Stanley, Nonlinear solutions of renormalization-group equations, *Phys. Rev. Lett.,* 32, 1446, 1974.

Nicoll, J.F., T. Chang, and H.E. Stanley, Nonlinear crossover between critical and tricritical behavior, *Phys. Rev. Lett.,* 36, 113, 1976.

Pavlos, G.P., M.A. Athanasiu, D. Kugiumtzis, N. Hatzigeorgiu, A.G. Rigas, and E.T. Sarris, Nonlinear analysis of magnetospheric data Part I. Geometric characteristics of the AE index time series and comparison with nonlinear surrogate data, *Nonlinear Process Geophys.*, *6* (1), 51-65, 1999a.

Pavlos, G.P., D. Kugiumtzis, M.A. Athanasiu, N. Hatzigeorgiu, D. Diamantidis, and E.T. Sarris, Nonlinear analysis of magnetospheric data Part II. Dynamical characteristics of the AE index time series and comparison with nonlinear surrogate data, *Nonlinear Process Geophys.*, *6* (2), 79-98, 1999b.

Sergeev, V.A., K. Liou, C.I. Meng, P.T. Newell, M. Brittnacher, G. Parks, and G.D. Reeves, Development of auroral streamers in association with localized impulsive injections to the inner magnetotail, *Geophys. Res. Lett.*, *26* (3), 417-420, 1999.

Sharma, A.S., Assessing the Magnetospheres Nonlinear Behavior - Its Dimension Is Low, Its Predictability, *Rev. Geophys.*, 33, 645-650, 1995.

Tam, S.W.Y., T. Chang, S.C. Chapman, and N.W. Watkins, Analytical determination of power-law index for the Chapman et al., sandpile (FSOC) analog for magnetospheric activity -- a renormalization-group analysis, *Geophys. Res. Lett.,* 27, 1367, 2000a.

Tam, S.W.Y., T. Chang, G. Consolini, and P. de Michelis, Renormalization-group description and comparison with simulation results for Forest-Fire models -- possible

near-criticality phenomenon in the dynamics of space plasmas, *Trans. Amer. Geophys. Union*, *EOS*, 81, SM62A-04, 2000b.

Tetreault, D.J., Magnetohydrodynamic clump instability, *Physics of Fluids*, 31, 2122, 1988.

Tetreault, D.J., Steady-state magnetohydrodynamic clump turbulence, *Physics of Fluids*, B1, 511, 1989.

Tetreault, D., Turbulent relaxation of magnetic fields: 1. coarse-grained dissipation and reconnection, *J. Geophys. Res.*, 97, 8531, 1992a.

Tetreault, D., Theeory of electric fields in the auroral acceleration region, *J. Geophys. Res.*, 96, 3549, 1992b.

Uritsky, V.M., and M.I. Pudovkin, Low frequency 1/f-like fluctuations of the AE-index as a possible manifestation of self-organized criticality in the magnetosphere, *Ann. Geophys.*, *16* (12), 1580-1588, 1998.

Uritsky, V.M., A.J. Klimas, J.A. Valdivia, D. Vassiliadis, and D.N. Baker, Stable critical behavior and fast field annihilation in a magnetic field reversal model, *J. Atmos. Sol-Terr. Phy.*, *63* (13), 1425-1433, 2001a.

Uritsky, V.M., A.J. Klimas, and D. Vassiliadis, Multiscale dynamics and robust critical scaling in a continuum current sheet model, *Phys. Rev. E*, 65, 046113, 2002a.

Uritsky, V.M., A.J. Klimas, D. Vassiliadis, D. Chua, and G.D. Parks, Scale-free statistics of spatiotemporal auroral emissions as depicted by POLAR UVI images: The dynamic magnetosphere is an avalanching system, *J. Geophys. Res.*, submitted, 2002b.

Valdivia, J.A., A.S. Sharma, and K. Papadopoulos, Prediction of magnetic storms by nonlinear models, *Geophys. Res. Lett.*, *23* (21), 2899-2902, 1996.

Valdivia, J.A., D. Vassiliadis, A.J. Klimas, and A.S. Sharma, Modeling the spatial structure of the high latitude magnetic perturbations and the related current system, *Phys. Plasmas*, *6* (11), 4185-4194, 1999.

Vassiliadis, D., A.J. Klimas, D.N. Baker, and D.A. Roberts, A description of the solar-wind magnetosphere coupling based on nonlinear filters, *J. Geophys. Res.*, *100* (A3), 3495-3512, 1995.

Vassiliadis, D., A.J. Klimas, J.A. Valdivia, and D.N. Baker, The *Dst* geomagnetic response as a function of storm phase and amplitude and the solar wind electric field, *J. Geophys. Res.*, *104* (A11), 24957-24976, 1999.

Wilson, K.G. and J. Kogut, The renormalization group and the epsilon-expansion, *Physics Reports,* 12C, 76, 1974.

Wu, C.C., and T. Chang, 2D MHD Simulation of the Emergence and Merging of Coherent Structures, *Geophys. Res. Lett.,* 27, 863, 2000a.

Wu, C.C., and T. Chang, Dynamical evolution of coherent structures in intermittent two-dimensional MHD turbulence, *IEEE Trans. on Plasma Science*, 28, 1938, 2000b.

Wu, C.C., and T. Chang, "Further Study of the Dynamics of Two-Dimensional MHD Coherent Structures -- A Large Scale Simulation", *Journal of Atmospheric Sciences and Terrestrial Physics*, 63, 1447, 2001.

Zelenyi, L.M., A.V. Milovanov, and G. Zimbardo, Multiscale magnetic structure of the distant tail: self-consistent fractal approach, *AGU Monograph on "New Perspectives*

on the Earth's Magnetotail", ed. Nishida, A., D.N. Baker, and S.W.H. Cowley, American Geophysical Union, Washington, D.C., v. 105, p. 321, 1998.

III.2 Comparison of the effects of wave-particle interactions and the kinetic suprathermal electron population on the acceleration of the solar wind

III.2.1 Introduction

Since the pioneering work by *Belcher and Davis* [1971], the existence of waves has been well established in the research of the fast solar wind. Wave-particle interactions have been considered as a possible solar wind heating mechanism, and their effects have been studied by a number of authors [e.g. *Hollweg and Turner*, 1978; *Dusenbery and Hollweg*, 1981; *Marsch et al.*, 1982c; *Isenberg*, 1984; *Leer et al.*, 1982; *Hu et al.*, 1997; *Czechowski et al.*, 1998; *Cranmer et al.*, 1999b; *Hu and Habbal*, 1999; *Li et al.*, 1999, *Tam and Chang*, 1999a; *Isenberg et al.*, 2000; *Cranmer*, 2001; *Gary et al.*, 2001; *Liewer et al.*, 2001; *Tam and Chang*, 2001; *Tu and Marsch*, 2001; *Vocks and Marsch*, 2001]. Experimentally, there has been increasing evidence suggesting that wave-particle interactions play a significant role in the evolution and acceleration of the solar wind. First, the proton velocity distributions observed by the Helios spacecraft featured an anisotropy in the core region, where the temperature in the perpendicular direction was higher than that in the direction parallel to the magnetic field [*Marsch et al.*, 1982b]. Such an anisotropy was an indication of the presence of ion perpendicular heating in the solar wind. The observed proton velocity distributions were also frequently characterized by double peaks in the field-aligned direction. The formation of these double peaks has recently been associated with kinetic ion cyclotron resonances involving sunward propagating electromagnetic waves [*Tam and Chang*, 1999a,b].

The differential speeds between the alpha particles and the protons in the solar wind, which were perhaps the most unexpected experimental results observed by the Helios spacecraft, may also be highly related to wave-particle interactions. Measure-

ments by the spacecraft revealed that the helium ions have a higher outflow speed compared with the protons [*Marsch et al.*, 1982a], especially in the fast solar wind. Indeed, more recent observations by the WIND and the Ulysses spacecraft have also arrived at a similar conclusion [*Steinberg et al.*, 1996; *Feldman et al.*, 1996]. Because the helium ions have a smaller charge-to-mass ratio compared with the protons, the observed ion differential speeds were inconsistent with the idea of the field-aligned ambipolar electric field being the main solar wind acceleration mechanism. A physical mechanism that has been demonstrated to preferentially accelerate helium ions rather than protons is kinetic ion resonant heating by electromagnetic waves in the ion gyrofrequency range [*Tam and Chang*, 1999a,b]. These waves may be produced by the small-scale reconnections near the coronal region. Recently, *Chang* [2003] has suggested that such type of intermittent turbulence may be associated with the "complexity" generated by the sporadic localized mergings and interactions of the coherent magnetic structures near the coronal holes. Measurements of the power spectra of these waves by the Helios spacecraft indicated that the wave power decreases with frequency [*Bavassano et al.*, 1982; *Denskat and Neubauer*, 1982]. Note that the alpha particles have a lower gyrofrequency than the protons. Therefore, in general, more wave power is available to the helium ions than to the protons, at least in the observed regimes (0.3–1 AU). Extrapolating the power spectrum to distances close to the sun, *Tam and Chang* [1999a] have shown that the kinetic wave-particle interactions in general transfer more energy to a helium ion than to a proton. Although the energy is mainly transferred into the transverse direction, it converts into the field-aligned direction downstream in the solar wind due to the mirror effect, leading to a preferential acceleration of the helium ions.

Experimental data from SOHO have provided even more evidence in support of the significance of wave-particle interactions in the fast solar wind. The observed O^{5+}

ions in the extended corona deviate significantly from those of a thermal distribution. Their velocity distributions are strongly anisotropic, with $T_{\perp} > T_{||}$, and perpendicular kinetic temperature higher than 10^8 K [*Kohl et al.*, 1998; *Cranmer et al.*, 1998, 1999a]. It has been pointed out by the investigators who analyzed the data that this evidence is consistent with ion cyclotron resonant heating.

Besides wave-particle interactions, other physical mechanisms have also been considered as possible drivers of the solar wind. The proposal of suprathermal electron effects has led to theory-data agreement in the ionospheric polar wind, which, like the solar wind, is an outflow of space plasmas along open magnetic field lines. The reason why suprathermal electrons may drive an outflowing plasma, such as the solar wind, is the following. Without taking wave-particle interactions into consideration, *Scudder and Olbert* [1979] argued that due to the velocity-dependence of the Coulomb collisional depth and the global kinetic nature of the solar wind outflow, suprathermal tails could be formed in the electron distributions. To demonstrate this "velocity filtration effect", these authors used a simplified collisional operator to determine the evolution of an electron distribution along the solar wind. They were able to show that an electron distribution in the form of a Maxwellian at the corona could evolve into one with a notable tail population in the anti-sunward direction near 1 AU. *Olbert* [1982] further suggested that the heat flux contribution by the suprathermal electron tail may drive the solar wind. Such an idea has been applied to the ionospheric polar wind with photoelectrons playing the role of the suprathermal population [*Tam et al.*, 1995, 1998], and has successfully addressed the various features observed by satellites. It has been shown that in the absence of wave-particle interactions, the suprathermal electron population can increase the ambipolar electric field, leading to higher ion outflow speeds in the polar wind. Because the ionospheric polar wind and the solar wind are analogous phenomena — both are outflow of space plasmas along

open magnetic field lines — it is reasonable to expect that suprathermal electron effects may accelerate the ions in the solar wind.

The combined effects of ion cyclotron resonant heating and the suprathermal electron population have been considered in a solar wind study by *Tam and Chang* [1999a]. The study was the first to describe the global kinetic evolution and acceleration of the fast solar wind under the influence of the wave-particle interactions, Coulomb collisions, and an ambipolar electric field that was consistent with the particle distributions themselves. Results of the investigation associated the wave-particle interactions with some of the solar wind observations discussed earlier, including the differential speed between the helium ions and the protons, and the double-peaked proton velocity distributions. The bulk acceleration of the solar wind demonstrated in the study, however, consisted of contributions due to both the ion resonances and the suprathermal electron effects. It was therefore unclear to what extent each of the two acceleration mechanisms contributes to the driving of the solar wind. Our goal in this study is to compare the relative importance of the kinetic effects due to suprathermal electrons and ion cyclotron resonances, and to determine which of the acceleration mechanisms is mostly responsible for the driving of the solar wind.

III.2.2 Model

Our model in this study is based on a self-consistent hybrid technique originally developed to describe the ionospheric polar wind [*Tam et al.*, 1995, 1998]. Because the polar wind (as termed in analogy with the solar wind [*Axford*, 1968; *Banks and Holzer*, 1968]) is also an example of plasma outflow along open magnetic field lines, our present model retains the general features of the self-consistent hybrid model: It is based on an iterative scheme between fluid and kinetic calculations. In the fluid calculations, a set of equations determines the ambipolar electric field and the

properties of the bulk thermal electrons, whose distributions are assumed to be in a drifting Maxwellian. To solve the fluid equations, we impose the quasi-neutrality and current-free constraints for the solar wind, and make use of the results from the kinetic calculations in the model. The kinetic part of the model consists of multiple components, each describing the evolution of a particle component along the solar wind. In the basic version of the model, the kinetic approach is applied only to two particle components: proton and alpha particle, the two major ion species in the solar wind. The distributions of these ions evolve under the influence of Coulomb collisions, an ambipolar electric field, and wave-particle interactions. Results based on the global evolution of these distributions are coupled into the fluid calculations. This coupling ensures the consistency of the ambipolar electric field with the particle distributions when an iteration between the fluid and kinetic parts of the model converges. In addition, a convergence of the results enables our kinetic calculations to correctly take into account the Coulomb collisions for the ions, including those among the same ion species.

Effects of kinetic ion resonant heating are incorporated into the model with a Monte Carlo technique. This technique was originally developed to model ion resonant heating in the auroral region, and has successfully addressed the existence of ion conics [*Retterer et al.*, 1983]. By including this technique into the model, we are able to incorporate the resonant effect of a given wave spectrum into an otherwise self-consistent solar wind description.

To be more quantitative on the description of our kinetic calculations, we solve the following steady-state collisional kinetic equations for the protons and the helium ions, the particle components that resonate with the waves:

$$\left[v_{\|}\frac{\partial}{\partial s}-\left(g-\frac{q}{m}E_{\|}\right)\frac{\partial}{\partial v_{\|}}-{v_{\perp}}^{2}\frac{B'}{2B}\left(\frac{\partial}{\partial v_{\|}}-\frac{v_{\|}}{v_{\perp}}\frac{\partial}{\partial v_{\perp}}\right)\right]f_j=C_jf_j+D_jf_j, \quad \text{(III.2.1)}$$

where s is the distance along the radial magnetic field line, $v_{\|}$ and $v_{\perp}$ denote velocities

in the spacecraft frame, $f_j(s, v_\|, v_\perp)$ is the distribution function for the particle species j, q and m are the electric charge and mass of the species respectively, $E_\|$ is the field-aligned ambipolar electric field, g is the gravitational acceleration, B is the magnetic field, $B' \equiv dB/ds$, C_j is a Coulomb collisional operator for the species j, and

$$D_j = \frac{\partial}{\partial v_\|} D_{j\|} \frac{\partial}{\partial v_\|} + \frac{1}{v_\perp} \frac{\partial}{\partial v_\perp} \left(v_\perp D_{j\perp} \frac{\partial}{\partial v_\perp} \right) \qquad \text{(III.2.2)}$$

is an operator that describes resonant heating, with $D_{j\|}$ and $D_{j\perp}$ being quasilinear diffusion coefficients that represent heating in the parallel and perpendicular directions respectively. The expressions for $D_{j\|}$ and $D_{j\perp}$, in general, depend on a number of factors, including the kind of wave-particle interactions, the conditions for resonances, the power of the waves, *etc.* Below, we discuss in detail the conditions that determine the diffusion coefficients in the study.

Ion Cyclotron Resonant Heating

The wave-particle interactions to be described in Eq. (III.2.1) and (III.2.2) are kinetic ion cyclotron resonances, which have been demonstrated to preferentially accelerate the helium ions over the protons [*Tam and Chang*, 1999a,b]. The resonances that we consider involve electromagnetic waves whose wavevector component $k_\perp \ll k_\| \approx k$. Because the thermal speeds of the ions are much smaller than the local Alfvén speed near the corona, where the majority of the resonant heating occurs, the properties of the waves can be approximated by a cold plasma dispersion relation. Moreover, due to the relatively low thermal speeds, few ions are able to resonate with right-hand polarized waves. Therefore, the only waves that we consider in this study are left-hand polarized, and are in the Alfvén/ion cyclotron branch, which in fact consists of two sub-branches for the two-ion (proton and helium) plasma in our model. In the solar wind frame, the lower sub-branch covers all frequencies up to the helium gyrofrequency, Ω_α. The upper sub-branch plateaus at the proton gyrofrequency Ω_p for large k, and its frequency limit at infinite wavelength is above Ω_α, leaving a gap

between the two sub-branches. For an ion (proton or alpha particle) with parallel velocity $v'_{\parallel}$ in the solar wind frame to resonate with the left-hand polarized waves, the following condition has to be satisfied:

$$\omega' - kv'_{\parallel} = \Omega, \tag{III.2.3}$$

where ω' is the wave frequency in the solar wind frame, and Ω is the gyrofrequency of the ion. The wave frequency observed by the spacecraft is Doppler-shifted to ω, given by:

$$\omega = \omega' + kU, \tag{III.2.4}$$

where U is the local solar wind speed. Note that the sign of k can be positive or negative, representing outward (anti-sunward) or inward (sunward) propagating waves respectively.

Although the waves in the solar wind propagate predominantly outward, a statistical analysis of the power spectra measured by the Helios spacecraft indicated that inward propagating waves constitute a considerable amount of power in both the fast and slow solar wind [*Tu and Marsch*, 1990]. The study showed that in the fast solar wind, the power of inward propagating waves (e_-) tends to approach its outward counterpart (e_+) as the radial distance increases. The results of the study motivated us to include inward propagating waves in our model. We assume the following relation for the wave power ratio in the interplanetary space:

$$e_-/e_+ = 1 - e^{-(s/3)^2}\ , \tag{III.2.5}$$

where s is the heliocentric distance in AU. Note that with Eq. (III.2.5), we assume that the inward propagating waves constitute only 2.4×10^{-6} of the total wave power at 1 $R_\odot$ (solar radius). Even with such a small ratio of e_-/e_+ near the corona, the presence of these sunward propagating waves have been shown to lead to double-peaked proton velocity distributions in the solar wind [*Tam and Chang*, 1999a]. The reason for the formation of the non-thermal feature is as follows. Because $\omega' < \Omega_p$ for

all the waves in the ion cyclotron branch, it is clear from Eq. (III.2.3) that protons with $v'_{\|} < 0$ can only resonate with the outward propagating waves, while those with $v'_{\|} > 0$ only interact with the incoming waves. Note that at any given distance, the anti-sunward and sunward propagating waves heat two distinct proton populations in the velocity space. If incoming waves were absent, pitch-angle diffusion of the protons due to the wave-particle interactions could only occur at velocity space where $v'_{\|} < 0$. The presence of sunward propagating waves enables the proton distributions to undergo two distinct sets of pitch-angle diffusion, one at $v'_{\|} < 0$ and the other at $v'_{\|} > 0$. As the solar wind evolves along the flow, each of these two sets of velocity-space diffusion gives rise to a hump in the proton distributions because of the effect of mirror folding, thereby forming the observed double-peaked feature. Later, we shall provide evidence to support the association between double-peaked proton velocity distributions and sunward propagating waves when we briefly discuss the effect on the solar wind due to a different e_-/e_+ ratio.

The power of the waves in the solar wind decreases with frequency, as indicated by the Helios measurements of the magnetic field spectra [*Bavassano et al.*, 1982; *Denskat and Neubauer*, 1982]. The dependence of the wave power on frequency can generally be described by a power law. It was also found that the wave power decreases with radial distance, and the dependence can also be described by a power law, at least in the observed regime [*Bavassano et al.*, 1982]. In our model, we assume a magnetic field power spectrum based on these experimental results. We extend the power-law relation to higher frequencies. As for the dependence on radial distance, we assume a power-law relation and interpolate to obtain the magnetic field power between the two experimental limits (0.29 and 0.87 AU). For radial distances outside the measurement range, we assume the wave power to be proportional to $s^{-4.2}$.

With the resonance condition and magnetic field power spectra defined, we are

able to determine the frequencies and power of the waves that are in resonance with the ions. The two-ion (proton and helium) cold plasma dispersion relation for the left-hand polarized waves in the solar wind frame, which we consider to be the frame where both the combined ion populations and the total electron population carry zero current, can be expressed as:

$$(k\,v_A)^2 = \omega'^2 \left[\frac{1 - \omega'/\omega_0}{(1 - \omega'/\Omega_\alpha)(1 - \omega'/\Omega_p)} \right], \tag{III.2.6}$$

where v_A is the Alfvén speed, and

$$\omega_0 = \Omega_\alpha (n_p + 4n_\alpha)/(n_p + 2n_\alpha) \tag{III.2.7}$$

is a frequency that depends on the densities of the protons (n_p) and the helium ions (n_α). Note that ω_0 represents the long-wavelength limit for the upper ion cyclotron sub-branch. One can see that Eq. (III.2.6) does not have any solution for $\Omega_\alpha < \omega' < \omega_0$, resulting in a frequency gap between the two ion cyclotron sub-branches. However, in the limit of a one-ion plasma ($n_\alpha \to 0$), the frequency gap disappears (as $\omega_0 \to \Omega_\alpha$ in Eq. (III.2.7)), and the dispersion relation reduces to a single branch. Equation (III.2.6), together with Eq. (III.2.3), determine the wavevectors and frequencies of the waves that resonate with the individual ions in the solar wind frame. These resonant frequencies are then Doppler-shifted to the spacecraft frame according to Eq. (III.2.4). The total wave power at these frequencies are then determined based on the interpolation/extrapolation scheme of the magnetic field spectrum described earlier.

The diffusion coefficients in Eq. (III.2.2) involve all of the considerations discussed above. Standard expressions for these coefficients can be found in, for example, *Swanson* [1989]. But by taking into account all the considerations above, we arrive at a modified version of the diffusion coefficients:

$$D_{\|} = \eta \frac{q^2}{4m^2} \int d\omega\, v_\perp{}^2 P_B(\omega/2\pi)\, \delta(\omega - kv_{\|} - \Omega), \tag{III.2.8}$$

$$D_\perp = \eta \frac{q^2}{4m^2} \int d\omega\, (\Omega/k)^2 P_B(\omega/2\pi)\, \delta(\omega - kv_\parallel - \Omega), \tag{III.2.9}$$

where the δ-functions reflect our emphasis on the resonance condition equivalent to Eq. (III.2.3), ω and k are related through Eq. (III.2.3), (III.2.4) and (III.2.6), P_B is a function for the magnetic field wave power, which is based on our interpolation/extrapolation scheme of the Helios measurements, and depends on the sign of k (direction of the wave propagation) as described earlier, and lastly,

$$\eta = \eta_0 \exp\left[(1-r)/0.5\right] \tag{III.2.10}$$

is an efficiency factor that adjusts the available wave power, and depends on the heliocentric distance r (in the unit of $R_\odot$). The adjustment of the wave power is mainly for two reasons. First, the factor η_0 in Eq. (III.2.10) accounts for the fact that the left-hand circularly polarized waves constitute only a fraction of the total observed wave power. Second, the remaining factor on the right-hand side of the equation approximates the dissipation of the waves as they propagate along the magnetic field line from the sun. It is chosen based on the study by *Cranmer et al.* [1999b], who suggested that most of the waves originating from the solar surface are dissipated before reaching 1.5 $R_\odot$.

Kinetic Suprathermal Electron Effects

Up to this point, we have described the basic constituents of our model. This model enables us to follow the global evolution of the ion distributions along the solar wind flow, while taking into account the influence due to kinetic ion cyclotron resonant heating, Coulomb collisions, and an ambipolar electric field that is consistent with the particle distributions themselves. The kinetic effects of the ions are also incorporated into the overall solar wind picture through the coupling of their results with the fluid calculations. In fact, our modeling technique can readily incorporate the kinetic effects of another particle component. To do so, we simply add another kinetic component into the model to describe the particle population, and modify the

quasi-neutrality and current-free conditions, as well as the fluid equations accordingly. This flexibility makes our model an ideal tool to investigate the global kinetic effects of suprathermal electrons on the solar wind.

To take into account the global kinetic effects of the suprathermal electrons, we solve a steady-state collisional kinetic equation for the population that comprises the tail portion of the electron Maxwellian distribution at the lower boundary of our model. The equation is similar to Eq. (III.2.1), but without the term that represents wave-particle interactions. In addition, the operator that describes the Coulomb collisions for the suprathermal electrons is simplified. The collisional operator in Eq. (III.2.1), such as the Fokker-Planck collisional operator, should have the following expression in its complete form [see, e.g., *Ichimaru*, 1973; *Book*, 1989]:

$$C_j f_j(\mathbf{v}) = -\sum_b \nabla_{\mathbf{v}} \cdot \mathbf{J_{jb}}, \tag{III.2.11}$$

where the subscript b represents the background species with which the particles of species j interact, and

$$\begin{aligned} \mathbf{J_{jb}}(\mathbf{v}) = 2\pi\Lambda_{jb} \ \frac{q^2 {q_b}^2}{m} \int d^3v' \frac{(\mathbf{v}'-\mathbf{v})^2\mathbf{I} - (\mathbf{v}'-\mathbf{v})(\mathbf{v}'-\mathbf{v})}{|\mathbf{v}'-\mathbf{v}|^3} \\ \cdot \left[\frac{1}{m_b} f_j \nabla_{\mathbf{v}'} f_b(\mathbf{v}') - \frac{1}{m} f_b(\mathbf{v}') \nabla_{\mathbf{v}} f_j\right], \end{aligned} \tag{III.2.12}$$

where Λ_{jb} is the Coulomb logarithm, and $\mathbf{I}$ is the unit dyad. In the full collisional description, such as that for the ions, the background includes the thermal electrons and the two major ion species. But for the suprathermal electrons, we take into account their Coulomb interaction only with the thermal electrons. The interaction among the suprathermal electrons themselves are not considered due to their low relative density. With these approximations, and the assumption that the background thermal electron distribution is in the form of a drifting Maxwellian,

$$f_e(\mathbf{v}) = n_e \left(\frac{m_e}{2\pi T_e}\right)^{3/2} \exp\left[-\frac{m_e(\mathbf{v}-\mathbf{u_e})^2}{2T_e}\right], \tag{III.2.13}$$

the collisional term in the kinetic equation for the suprathermal electrons becomes:

$$C_s f_s = -\nabla_{\mathbf{v}} \cdot (\mathbf{a}_{\text{coll,s}} f_s) + \nabla_{\mathbf{v}} \cdot (\mathbf{D}_{\text{coll,s}} \cdot \nabla_{\mathbf{v}} f_s), \tag{III.2.14}$$

where

$$\mathbf{a}_{\rm coll,s} = -(m_s/m_e)\,\nu_0\,\mathbf{c}\,\Psi(x_e), \tag{III.2.15}$$

$$\mathbf{D}_{\rm coll,s} = \frac{\nu_0}{2}\,\mathbf{c}\,\mathbf{c}\,\frac{\Psi(x_e)}{x_e} + \frac{\nu_0}{2}\,(c^2\mathbf{I} - \mathbf{c}\,\mathbf{c})\Big[\Big(1 - \frac{1}{2x_e}\Big)\,\Psi(x_e) + \Psi'(x_e)\Big], \tag{III.2.16}$$

with

$$\mathbf{c} = \mathbf{v} - \mathbf{u_e}, \tag{III.2.17}$$

$$\nu_0 = 4\pi\Lambda_{se} n_e {q_s}^2 {q_e}^2/{m_s}^2 c^3, \tag{III.2.18}$$

$$x_e \equiv m_e c^2/2T_e, \tag{III.2.19}$$

$$\Psi(x) = \frac{2}{\sqrt{\pi}}\int_0^x dt\sqrt{t}\,e^{-t}, \tag{III.2.20}$$

$\Psi'(x) \equiv d\Psi/dx$, and the subscripts s and e stand for the suprathermal and thermal electrons respectively (thus, $q_s = q_e$ and $m_s = m_e$). Equation (III.2.14) indicates that the Coulomb collisions have two effects on the suprathermal electrons: to provide a deceleration and a diffusion. The expression for $\mathbf{a}_{\rm coll,s}$ in Eq. (III.2.15) suggests that the collisions act as a friction between the thermal electrons and the individual suprathermal electrons. The Coulomb interaction also leads to a diffusion of the suprathermal electrons in the velocity space, characterized by the tensor $\mathbf{D}_{\rm coll,s}$. Note that mathematically, $\mathbf{D}_{\rm coll,s}$ plays a similar role as $D_{j\parallel}$ and $D_{j\perp}$ of Eq. (III.2.2) in the governing kinetic equation. Therefore, the Monte Carlo technique in our model can also describe the diffusion due to the Coulomb collisions. According to Eq. (III.2.15) and (III.2.16), both the diffusion and the friction are characterized by a collisional frequency ν_0. Because ν_0 is proportional to $1/c^3$ (see Eq. (III.2.18)), the more energetic suprathermal electrons are less collisional. Because of this relationship, Coulomb collisions are expected to enhance the tail portion of the total electron distribution as the particles travel downstream along the solar wind flow. In our model, the electrons at the tail portion of the distribution have to satisfy two criteria at 1 $R_\odot$, the lower boundary in the calculations, in order to be considered suprathermal: $(1/2)m_e v^2 > 8T_{e0}$ and $v_\parallel > 0$, where T_{e0} is the thermal electron temperature at 1 $R_\odot$.

With the kinetic effects of suprathermal electrons being considered, the total electron distributions can no longer be in the form of a drifting Maxwellian. The distributions are now formed by the combination of a drifting Maxwellian for the thermal electrons, and the results from the kinetic calculations for the suprathermal electrons. As in the basic version of the model, the various parameters that constitute the drifting Maxwellian distributions for the thermal electrons – as well as the ambipolar electric field – are determined in the fluid calculations.

The density and drift velocity of the thermal electrons are determined from the quasi-neutrality and current-free constraints that characterize the solar wind, with input of densities and flow velocities of the other particle components (proton, helium, and suprathermal electron) obtained from the kinetic part of the model. In particular, the current-free condition is:

$$n_e u_e + n_s u_s = n_p u_p + 2 n_\alpha u_\alpha, \tag{III.2.21}$$

where the subscripts p, and α stand for the protons and the alpha particles respectively. The density and drift velocity profiles of the thermal electrons (and in fact, of every plasma component) should also satisfy the continuity equation:

$$\frac{\partial}{\partial s}\left(\frac{nu}{B}\right) = 0. \tag{III.2.22}$$

However, note that both Eq. (III.2.21) and (III.2.22) involve the number flux of the particle species. Because the profiles of the particle components obtained from the kinetic part of the model have already satisfied Eq. (III.2.22), the imposition of the current-free constraint throughout the whole simulation range renders thermal electron density and velocity profiles that would also satisfy Eq. (III.2.22).

The thermal electron temperature, together with the ambipolar electric field, are obtained from the moment equations of the next two higher orders, *i.e.* the momentum and energy transfer equations for the whole electron population:

$$B\frac{\partial}{\partial s}\left(\frac{n_eT_e + n_e m_e {u_e}^2 + n_s T_{s\|} + n_s m_e {u_s}^2}{B}\right) + (n_e+n_s)\left(m_e\frac{\partial \Phi_G}{\partial s} - e\frac{\partial \Phi_E}{\partial s}\right)$$

$$+\frac{B'}{B}(n_eT_e + n_sT_{s\perp}) = \frac{\delta M_e}{\delta t} + \frac{\delta M_s}{\delta t}, \qquad \text{(III.2.23)}$$

$$B\frac{\partial}{\partial s}\left[\frac{n_e u_e}{B}\left(\frac{5}{2}T_e + \frac{m_e {u_e}^2}{2}\right) + \frac{Q_{w,s}}{B} + \left(\frac{n_e u_e}{B} + \frac{n_s u_s}{B}\right)(m_e\Phi_G - e\Phi_E)\right]$$

$$= \frac{\delta E_e}{\delta t} + \frac{\delta E_s}{\delta t} \qquad \text{(III.2.24)}$$

where e is the elementary charge, Φ_G is the gravitational potential, Φ_E is the potential for the field-aligned ambipolar electric field, $Q_{w,s}$ is the energy flux of the suprathermal electron population, obtained from the kinetic calculations, and $\delta M_{e,s}/\delta t$ and $\delta E_{e,s}/\delta t$ represent the rates of momentum and energy transfers to the thermal and suprathermal electrons due to Coulomb collisions. Unlike the standard moment method [*Schunk*, 1977], where the collisional transfer values are completely based on assumed distribution functions, such as a Maxwellian, the rates of momentum and energy transfers in Eq. (III.2.23) and (III.2.24) are determined based on the results of the kinetic components of our model. By calculating the momentum and energy transferred to the ions from the electrons in our kinetic simulations, we find these collisional transfer values with momentum and energy conservation, which results from the anti-symmetries of the Coulomb collisional operator in Eq. (III.2.12). However, we should note that the suprathermal electrons are not included in the collisional background for the ions. Nor are the ions included in the collisional background for the suprathermal electrons. These collisional values, therefore, do not take into account the transfer between the ions and the suprathermal electrons. *Fichtner et al.* [1996] studied the collisional transfers based on a number of distribution functions. Their results indicated that the transfer values for some non-Maxwellian distributions could be significantly different from those for a Maxwellian. However, they also noted that for distributions whose core regions do not deviate significantly from a Maxwellian, their collisional transfer values are similar to the Maxwellian case. As we shall show,

the suprathermal electrons in our calculations do not significantly affect the core of the total electron distributions. Therefore, we believe that the transfer values due to collisions between the suprathermal electrons and the ions are negligible.

We note that the formulation of the fluid calculations is simpler when the kinetic effects of suprathermal electrons are not considered. In that case, the total electron distributions consist only of the thermal electrons, and, by assumption, are in the form of a drifting Maxwellian. One may then drop all the terms with subscript s in Eq. (III.2.21), (III.2.23) and (III.2.24) to recover the fluid equations. However, whether suprathermal electron effects are considered or not, when the results of both the fluid and kinetic parts of our model converge, not only the collisional operators in the kinetic calculations provide a self-consistent background for the Coulomb interactions of the ions, but the ambipolar electric field is also consistent with the particle distributions themselves. Convergence of the results thus renders physically meaningful solutions for our solar wind model.

III.2.3 Comparison of Solar Wind Driving Mechanisms

Strong Wave-Driven Case

As discussed, we can incorporate the suprathermal electron effects into our solar wind model by including the optional kinetic component described in Section III.2.2. Because interactions between the electrons and the waves are not considered, the kinetic suprathermal electron effects in our calculations are essentially the velocity filtration effect proposed by *Scudder and Olbert* [1979]. Thus, by comparing solutions generated with and without the optional suprathermal electron component being included, we can identify the contribution by the velocity filtration effect in driving the solar wind.

We have generated two such solar wind solutions for the range between 1 $R_\odot$

and 1 AU with identical parameters and boundary conditions. The interplanetary magnetic field that we use is based on a dipole + quadrupole + current sheet model [*Banaszkiewicz et al.*, 1998]:

$$B(r) = 2.21\left[\frac{2}{(r/R_\odot)^3} + \frac{4.5}{(r/R_\odot)^5} + \frac{1}{1.538(r/R_\odot + 1.538)^2}\right] \text{ Gauss.} \quad \text{(III.2.25)}$$

Boundary and initial conditions are imposed at the lower end of the calculations: a thermal electron temperature of 100 eV is assumed. Initial velocity distributions for the protons and helium ions are the upper halves of Maxwellian distributions, whose temperatures are also 100 eV. The proton and helium ion densities are respectively 4.2×10^7 and 4.0×10^6 cm^{-3}. The parameter η_0 that characterizes the strength of the available wave power is 0.016. As we shall discuss below, such a value for η_0 corresponds to the case of a strong wave-driven solar wind.

Comparing the two solar wind solutions, we find that the most noticeably different results are the shape of the total electron distributions. Although in both cases we begin with a total electron distribution in the form of a Maxwellian at 1 $R_\odot$, we find that the distributions become different downstream in the flow. Figure III.2.1 shows the total electron distributions at two different locations. At 0.1 AU, in the solution where global kinetic effects are considered for the suprathermal electrons, a significant tail in the outward portion of the total electron distribution has already been developed. Downstream in the solar wind, even though the temperature of the thermal electrons is reduced, the tail remains as strong (middle panel of Fig.III.2.1). Thus, relative to the thermal core, the tail portion of the electron distribution is more enhanced downstream. The formation and enhancement of this non-thermal feature verify Scudder and Olbert's [1979] idea of the velocity filtration effect.

The deviation of the total electron distribution from the Maxwellian approximation can be seen more clearly in the bottom panel of Fig.III.2.1, where the reduced distributions in the parallel direction for the two solutions are shown. It is evident

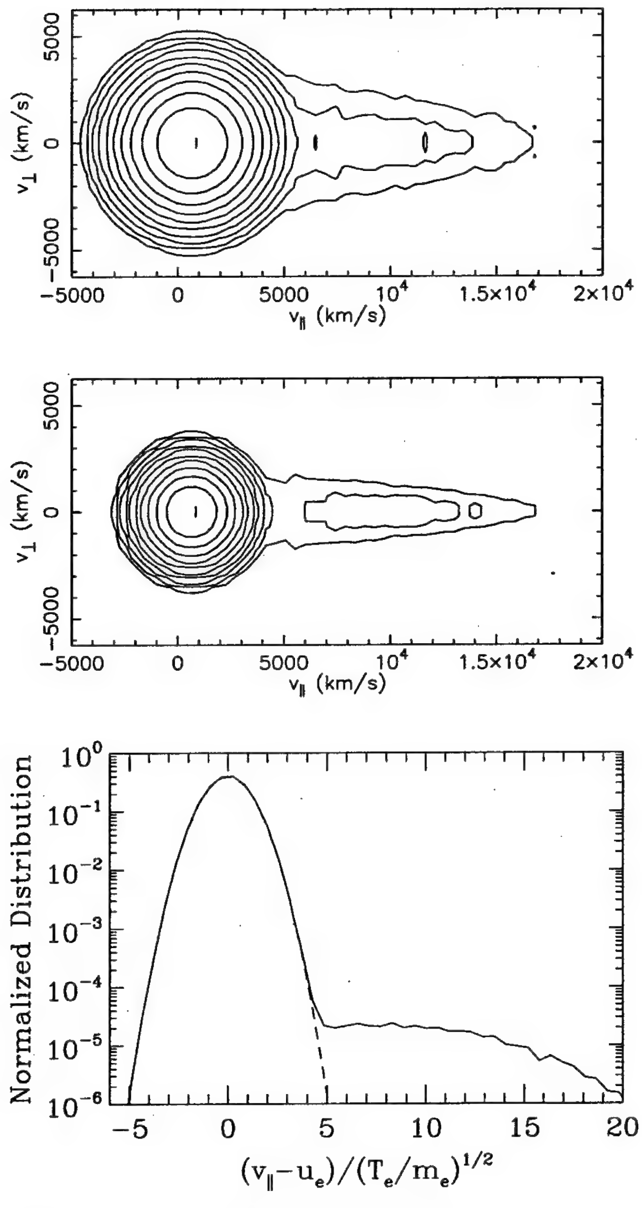

Figure III.2.1: Top and middle panels: Contour plots for the total electron distributions at 0.1 AU (top) and 0.4 AU (middle) for the case that includes suprathermal electrons. Bottom panel: Reduced electron distributions in the parallel direction at 0.4 AU. Solid line is the distribution for the case where global kinetic effects of the suprathermal electrons are included. Dashed line is the result with a Maxwellian approximation for the entire electron population.

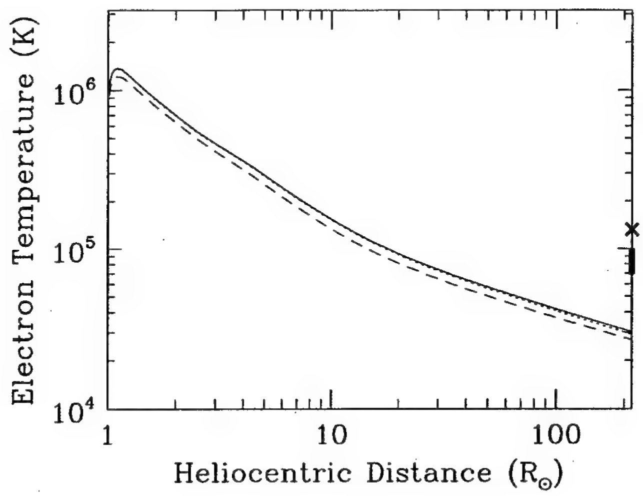

Figure III.2.2: Solid (dotted) line: Parallel (perpendicular) temperature of the total electron population for the case where global kinetic effects of the suprathermal electrons are included. Dashed line: Electron temperature for the Maxwellian approximation. The thick line segment and the cross ($\times$) at the right of the plot correspond to the core electron temperatures observed by the Helios [*Pilipp et al.*, 1990] and Ulysses [*Scime et al.*, 1994] spacecraft respectively.

that while the suprathermal electrons have a very significant contribution in the tail portion of the distribution, they do not really affect the core region. In fact, by comparing the overall electron temperature in the two solutions, we find that the suprathermal electrons do not affect the results by a significant amount (Fig. III.2.2). Therefore, our test-particle approximation for the suprathermal electrons regarding their Coulomb collisions seems reasonable.

The formation of the suprathermal tail in the electron distributions leads to an outward total electron heat flux throughout the solar wind, as opposed to a zero heat flux with a Maxwellian approximation. As shown in Fig. III.2.3, the profile of this outward electron heat flux essentially follows a power law from beyond 10 $R_\odot$ ($\approx$ 0.05 AU). Although the heat flux profile has a power-law index of -2.06, which seems to agree with the estimates based on a number of fast solar wind events observed by the Helios spacecraft [*Pilipp et al.*, 1990], its value at 1 AU, like the electron temperature, is about an order of magnitude too low compared with the observations

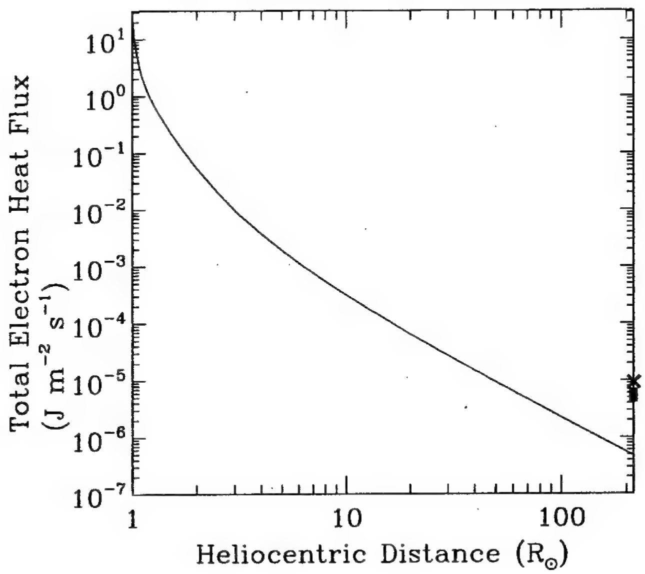

Figure III.2.3: Profile of the total electron heat flux from 1 $R_\odot$ to 1 AU in the case where the kinetic effects of the suprathermal electrons are included. The meaning of the thick line segment and the cross ($\times$) is similar to that in Fig. III.2.2.

(see Fig. III.2.2 and III.2.3). However, it has been shown that kinetic wave-particle interactions involving the solar wind electrons can increase the temperature and the heat flux of the species remarkably [*Tam and Chang*, 2001]. In the present study, we exclude the electron heating so as to present a clearer picture of the impact by the velocity filtration effect.

The suprathermal electron population influences the ion species mainly through the ambipolar electric field. The ambipolar electric potential profiles for the two solar wind solutions are shown in Fig. III.2.4. With a Maxwellian approximation for the entire electron population, the overall electric potential drop is about 700 V from 1 $R_\odot$ to 1 AU. The potential difference increases by about 70 V when kinetic suprathermal electron effects are taken into account. Such an increase suggests that the velocity filtration effect can accelerate the ions in the solar wind.

To evaluate the significance of the velocity filtration effect as a solar wind driving mechanism, we shall compare its contribution with those from other physical mecha-

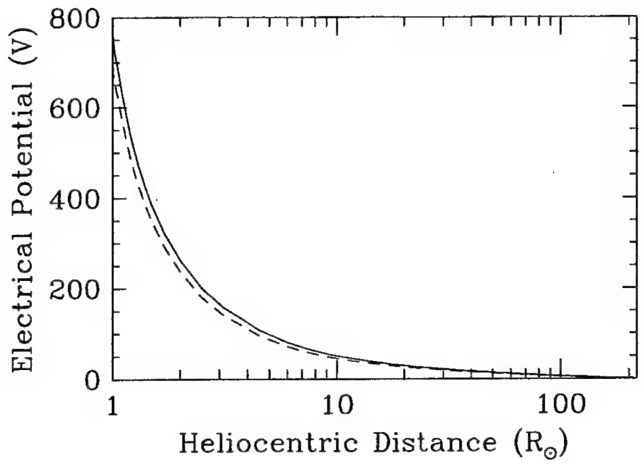

Figure III.2.4: Ambipolar electric potential profiles. Solid line: kinetic suprathermal electron effects included; dashed line: with a Maxwellian approximation for the entire electron distribution.

nisms in terms of energy input to the ion populations. Besides the kinetic effect that associates with the suprathermal electrons, there are several physical processes affecting the ion energy in the solar wind. First, ion cyclotron resonant heating provides a direct source of energy input for both the protons and helium ions. In addition, Coulomb collisions allow energy exchange between different species in the solar wind. The energies of the ions are affected by these two physical processes not only directly, but also indirectly through the influence of these mechanisms on the ambipolar electric field. As the ions travel downstream along the solar wind flow, their kinetic energy increases due to the sunward gradient of the ambipolar electric potential (see Fig. III.2.4), but at the same time, some of the kinetic energy is converted into gravitational potential energy. Whether an ion can reach large radial distances in the solar wind depends whether the kinetic energy it gains is high enough to overcome the gravitational potential. Therefore, we evaluate the significance of a physical mechanism in driving the solar wind by comparing its contribution to the energy input for the ions with the contributions from all the physical processes combined. Because we are interested in comparing only the processes that may drive the solar wind, we shall ex-

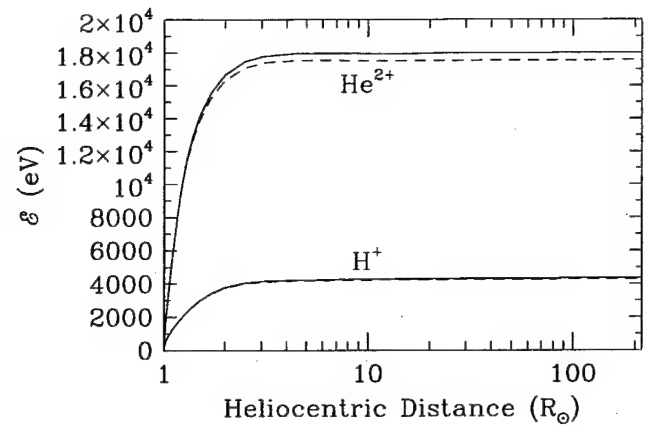

Figure III.2.5: $\mathcal{E}$ for protons and helium ions. Solid lines: kinetic suprathermal electron effects included; dashed lines: with a Maxwellian approximation for the entire electron distributions.

clude the gravitational force in our energy consideration. After all, the gravitational potential profile is invariant under all solar wind conditions, and is independent of the presence of other physical processes. Hence, we define the following quantity for each ion species for our purpose of energy comparison:

$$\mathcal{E} \equiv \text{average kinetic energy} + \text{gravitation potential energy per ion.}$$

For a given ion species in our model, its increase in $\mathcal{E}$ along the solar wind flow is due to a combination of energy input from the ambipolar electric field, wave-particle interactions, and Coulomb collisions with other species. In particular, the ambipolar electric field also reflects the influence due to wave-particle interactions, and Coulomb collisions, and, in the case where the kinetic suprathermal electron effects are included, the velocity filtration effect as well. The profiles of $\mathcal{E}$ for the protons and helium ions in our two solar wind solutions are shown in Fig. III.2.5. It appears from the figure that the difference in $\mathcal{E}$ is very small between the two solutions. Indeed, we find that with the kinetic effects of the suprathermal electrons taken into account, the increase in $\mathcal{E}$ for the protons from 1 $R_\odot$ to 1 AU is only 1.5% larger than in the case of a Maxwellian approximation. For the helium ions, the corresponding difference is 2.4%.

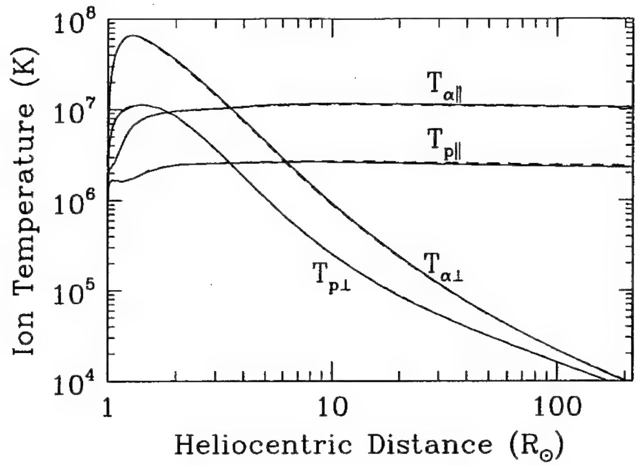

Figure III.2.6: Ion temperature profiles. Solid lines: kinetic suprathermal electron effects included; dashed lines: with a Maxwellian approximation for the entire electron distributions.

Because the quantity $\mathcal{E}$ characterizes the average kinetic energy, it is related to both the temperature and average outflow speed of the species. The temperature profiles of the ions in the two solar wind solutions are compared in Fig. III.2.6. One can see from the figure that the influence on the proton and helium ion temperatures due to the velocity filtration effect is negligible.

The influence by the kinetic suprathermal electron effects on the ion outflow speeds can be seen in Fig. III.2.7. The difference due to the velocity filtration effect is minimal, considering that the kinetic effect only lead to a 1.5% increase in the proton speed and a 2.3% increase in the helium ion speed at 1 AU. Note that even under a Maxwellian approximation for the overall electron distributions, the solar wind speed at 1 AU is as high as 650 km/s in the solution. Thus, the available wave power alone in these calculations seems to be able to drive the solar wind velocity to the high-speed range. Because of that, these solutions correspond to the case of a strong wave-driven solar wind.

As the ions in the two solar wind solutions have similar energies, outflow speeds, and temperatures, their velocity distributions are also similar. Fig. III.2.8 shows the

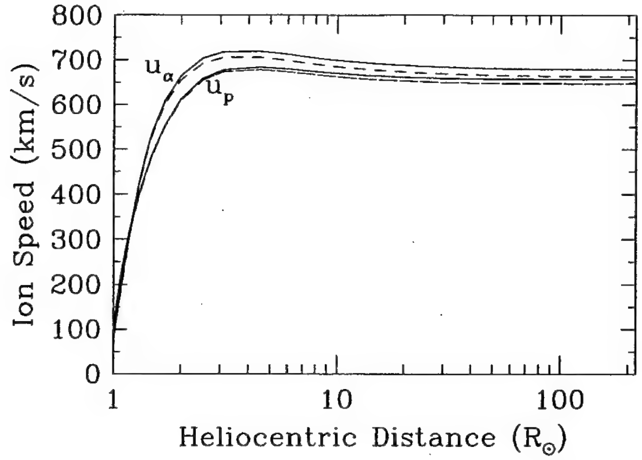

Figure III.2.7: Profiles of the proton and helium ion outflow speeds. Solid lines: kinetic suprathermal electron effects included; dashed lines: with a Maxwellian approximation for the entire electron distributions.

cuts of the normalized proton velocity distributions at the $v_\perp = 0$ plane of these strong wave-driven solutions. We can see that the distributions of the two solutions do not show a significant difference (open circles and crosses in Fig. III.2.8). For these solutions, there are no clear indications of a secondary peak. We have generated a different strong wave-driven solution with kinetic suprathermal electron effects considered. The parameters of this solution are identical to the cases discussed above, except that the ratio of sunward to anti-sunward propagating wave power, instead of Eq. (III.2.5), is replaced by the following expression:

$$e_-/e_+ = 1 - e^{-s^2} \ . \tag{III.2.26}$$

As shown in Fig. III.2.9, e_-/e_+ is larger by about an order of magnitude with Eq. (III.2.26) replacing Eq. (III.2.5). The increase in the sunward propagating wave power does not seem to affect the core region of the proton velocity distributions by much, as indicated in Fig. III.2.8. However, it has a stronger effect on the tail of the distributions. With the increase e_-/e_+ ratio, indications of the formation of a secondary peak at the tail are much stronger (filled circles in Fig. III.2.8). This result supports the association between double-peaked proton velocity distributions

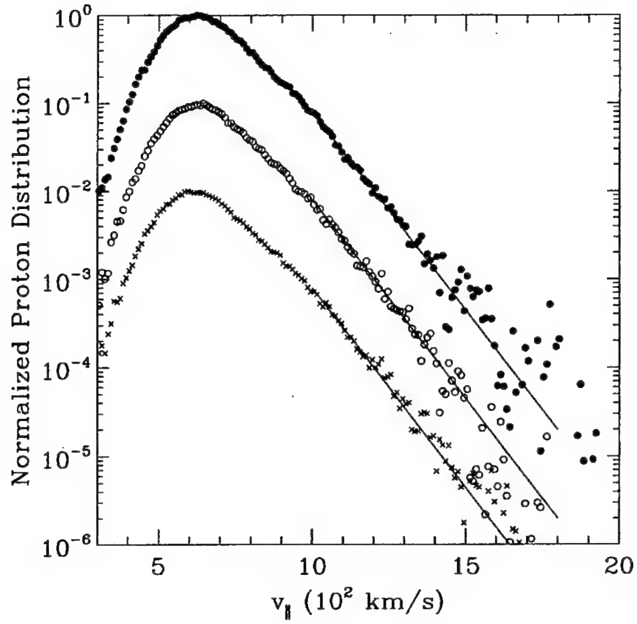

Figure III.2.8: Cuts of normalized proton velocity distributions at the $v_\perp = 0$ plane at 0.2 AU. The crosses ($\times$) corresponds to the solution based on a Maxwellian approximation for the total electron population. Open circles ($\circ$) are for the solution that includes kinetic suprathermal electron effects. The ratio e_-/e_+ is given by Eq. (III.2.5) for both of these cases. Filled circles ($\bullet$) are for e_-/e_+ given by Eq. (III.2.26), with suprathermal electron effects considered. For clarity, the distributions are normalized differently so that their peak values are exactly one order of magnitude apart. The straight solid lines at the tail of the distributions are parallel and also exactly one order of magnitude apart.

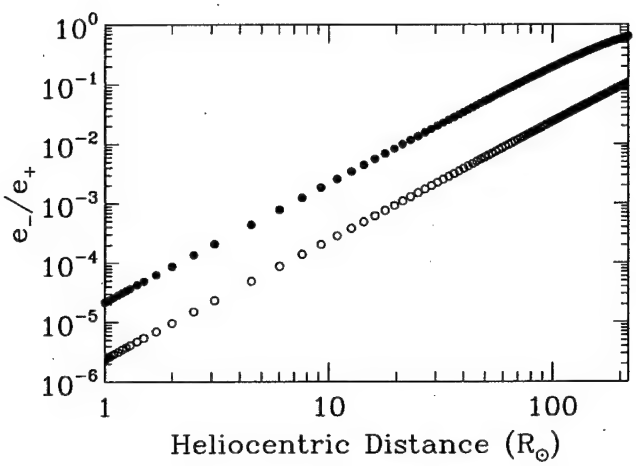

Figure III.2.9: The ratio of sunward to anti-sunward propagating wave power. Open circles: based on Eq. (III.2.5); filled circles: based on Eq. (III.2.26).

and sunward propagating waves that was discussed earlier.

Overall, it is clear from our comparison of the ion energies, outflow speeds, temperatures, and distributions that when strong wave-particle interactions are present, the velocity filtration effect plays an insignificant role in the driving and acceleration of the solar wind. Recently, *Vocks and Marsch* [2001, 2002] have introduced a semi-kinetic model for the solar wind to describe the effects of strong ion cyclotron resonant heating. Like this study, their model describes the wave-particle interactions in the framework of quasilinear theory. However, the treatment of the particles is different in the two models. Their model is based on reduced ion distributions, massless electron fluid, and an assumed electron temperature profile. With the approximations on the electrons, the model does not take into account the kinetic effects associated with the suprathermal electrons. However, as we have shown that the velocity filtration effect associated with the suprathermal electrons is negligible when strong ion resonant heating is present, Vocks and Marsch's assumptions regarding the electrons seem to be reasonable approximations.

Weak Wave-Driven Case

Kinetic suprathermal electron effects were proposed to be a solar wind acceleration mechanism under the assumption that no wave-particle interactions were present [*Olbert*, 1982]. Therefore, it is worthwhile for us to investigate the velocity filtration effect in the scenario of a weak wave-driven solar wind. In this scenario, we assume that the available wave power for ion resonances is not sufficient to drive the outflow to the velocity range of the fast solar wind. We are interested in finding out whether the velocity filtration effect can make a considerable contribution in driving the solar wind in this situation.

We compare two solar wind solutions for a weak wave-driven case, one with the kinetic effects associated with the suprathermal electrons taken into account, and the

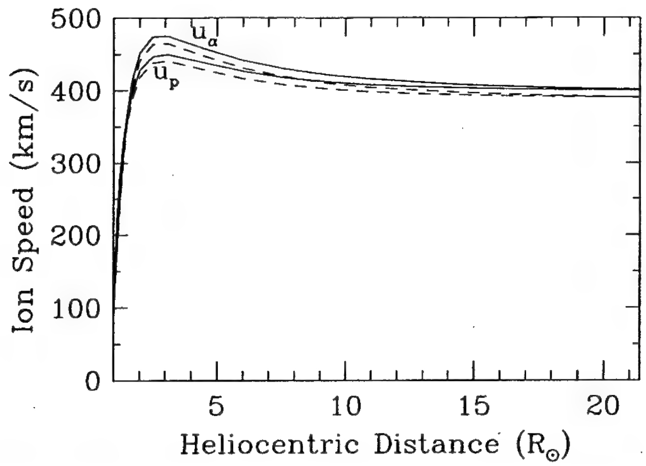

Figure III.2.10: Profiles of the proton and helium ion outflow speeds for the weak wave-driven solar wind case. Solid lines: kinetic suprathermal electron effects included; dashed lines: with a Maxwellian approximation for the entire electron distributions.

other with a Maxwellian approximation for the entire electron distribution. These calculations essentially share the same boundary conditions as those in the previous section, but with two exceptions. First, η_0 is reduced to 0.0075 to characterize the weak wave-driven scenario. Second, as indicated in Fig. III.2.5, the profiles for $\mathcal{E}$ have plateaued long before the distance reaches 1 AU. Therefore, for the present purpose, it is sufficient for us to set the upper boundary of the calculations to 0.1 AU ($\approx$ 21.5 $R_\odot$).

With the reduced level of available wave power, and without the suprathermal electron effects, we find that both the proton and helium ion speeds are only about 390 km/s at 0.1 AU (Fig. III.2.10). The inclusion of kinetic suprathermal electron effects increases these speeds only by 2.5% for the protons and 2.8% for the helium ions.

With the reduced wave power, the ion parallel temperatures, as shown in Fig. III.2.11, are smaller by about half compared with the corresponding values in the strong wave-driven solar wind case (Fig. III.2.6). However, as in the previous case, the velocity filtration effect does not seem to affect the ion temperature in the

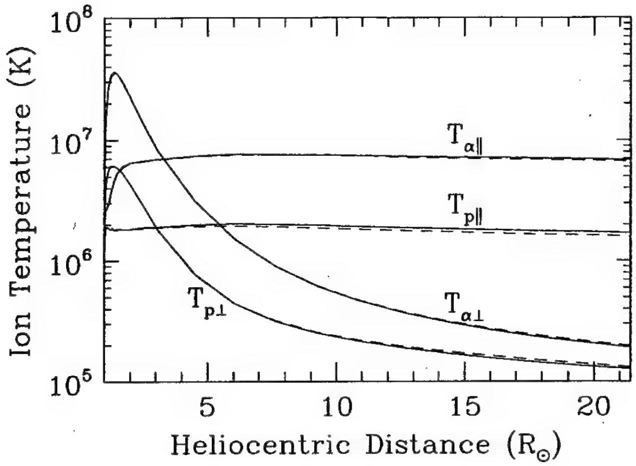

Figure III.2.11: Ion temperature profiles for the weak wave-driven solar wind case. Solid lines: kinetic suprathermal electron effects included; dashed lines: with a Maxwellian approximation for the entire electron distributions.

present scenario.

As for the energy quantity $\mathcal{E}$, comparison between Fig. III.2.5 and III.2.12 indicates that the values for both ion species reduce by about one-thirds due to the weaker wave power. By comparing the two solutions in Fig. III.2.12, one can see that with the reduced wave power, the velocity filtration effect is still only responsible for a small portion of the total energy input to the ions. For both ion species, inclusion of the

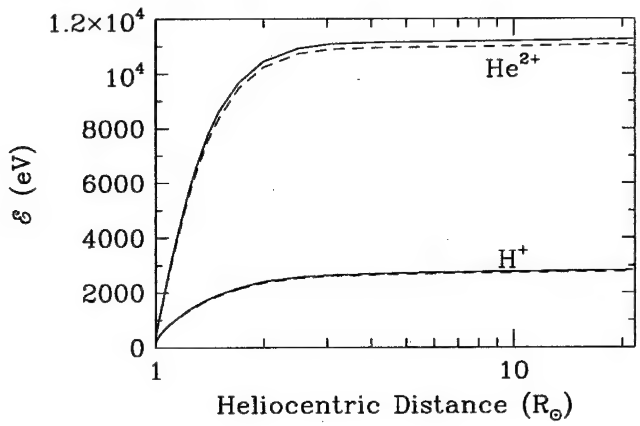

Figure III.2.12: $\mathcal{E}$ for protons and helium ions in the weak wave-driven solar wind scenario. Solid lines: kinetic suprathermal electron effects included; dashed lines: with a Maxwellian approximation for the entire electron distributions.

kinetic effect leads to an increase of less than 2% in the total energy input from 1 $R_\odot$ to 0.1 AU. Therefore, even in a weak wave-driven scenario, the velocity filtration effect is negligible in terms of driving and accelerating the solar wind.

III.2.4 Discussion

Our results have shown that ion cyclotron resonant heating is a much more efficient solar wind driving and acceleration mechanism compared with the velocity filtration effect that associates with the suprathermal electrons. Nevertheless, kinetic suprathermal electron effects, in general, may not always be negligible. In situations where there are physical processes which affect the suprathermal electron population more strongly than Coulomb collisions, kinetic suprathermal electron effects may contribute to the solar wind acceleration considerably. In fact, the strength of these kinetic effects depends on the electron distribution. We note that the suprathermal electrons considered in this study come from the tail portion of a Maxwellian distribution, whose temperature is 100 eV. Based on our experience, a higher electron temperature, due to the kinetic effects of the suprathermal electrons, would translate into a larger total electron heat flux. That would lead to a larger ambipolar electric field, and consequently, higher ion outflow speeds. Such a dependence between the electron temperature and the solar wind flow speed has been demonstrated by *Maksimovic et al.* [1997]. But perhaps more importantly, an electron distribution that deviates from the Maxwellian by having an enhanced suprathermal tail may affect the solar wind speed even more strongly. *Maksimovic et al.* [1997] and *Pierrard et al.* [1999] studied the effects of electron Kappa distributions on the solar wind from a few $R_\odot$ to 1 AU. They showed that in cases where the electron distributions had a very enhanced suprathermal tail, the solar wind velocities could approach the observed high-speed range. Although no physical processes were related to the possible for-

mation of such highly non-thermal electron distributions, these authors pointed out the association between a Kappa-like distribution near the corona and the observed electron distributions at 1 AU.

A physical mechanism that can significantly enhance the tail portion of the solar wind electron distributions, and increase the electron temperature and heat flux is wave-particle interactions. *Chashei and Fahr* [2000] suggested that electron heating due to, for example, preexisting whistler waves in the solar wind, is required to produce the electron heat flux observed by the Ulysses spacecraft. More recently, one of our studies [*Tam and Chang*, 2001] investigated the effects of electron cyclotron resonant heating in the solar wind. We showed that the electron heating by the right-hand polarized waves near the corona could raise the electron heat flux and temperature by an order of magnitude, and lead to a much larger ambipolar electric field due to the associated kinetic effects. The enhanced electric field resulted in a 16% increase in the proton outflow speed at 1 AU for the strong wave-driven case. Thus, even though ion resonant heating appears to be the dominant solar wind driving mechanism, the kinetic effects associated with the suprathermal electrons can sometimes make a considerable contribution to the acceleration of the solar wind.

III.2.5 Conclusions

In this study, we have compared the effects of two solar wind acceleration mechanisms: wave-particle interactions and the kinetic effects of the suprathermal electrons. Because the suprathermal electron population in our calculations corresponds to the tail portion of a Maxwellian distribution, it has been implicitly assumed that these suprathermal electrons have not undergone any heating, such as that involving electron cyclotron resonances. In addition, besides Coulomb collisions, we do not consider any physical process which may strongly affect the shape of the electron distributions.

Therefore, the kinetic suprathermal electron effects that we consider are essentially the velocity filtration effect, which arises due to Coulomb collisions and the global kinetic nature of the solar wind flow. Our results have shown that in the presence of ion cyclotron resonant heating, the contribution by the velocity filtration effect in the driving and acceleration of the solar wind is relatively insignificant. However, when there are other physical processes, such as electron cyclotron resonances, that strongly affect the suprathermal electrons, kinetic suprathermal electron effects may no longer be negligible.

References

Axford, W. I., The polar wind and the terrestrial helium budget, *J. Geophys. Res.*, **73**, 6855, 1968.

Banaszkiewicz, M., W. I. Axford, and J. F. McKenzie, An analytic solar magnetic field model, *Astron. Astrophys.*, **337**, 940, 1998.

Banks, P. M., and T. E. Holzer, The polar wind, *J. Geophys. Res.*, **73**, 6846, 1968.

Bavassano, B., M. Dobrowolny, F. Mariani, and N. F. Ness, Radial evolution of power spectra of interplanetary Alfvénic turbulence, *J. Geophys. Res.*, **87**, 3617, 1982.

Belcher, J. W., and L. Davis, Jr., Large-amplitude Alfvén waves in the interplanetary medium, 2, *J. Geophys. Res.*, **76**, 3534, 1971.

Book, D. L., Plasma physics, in *A Physicist's Desk Reference*, 2nd edn., ed. H. L. Anderson, American Institute of Physics, New York, p. 282, 1989.

Chang, T., "Complexity" induced plasma turbulence in coronal holes and the solar wind, to appear in the proceedings of Solar Wind 10, 2003.

Chashei, I. V., and H. J. Fahr, A thermokinetic study of wave-modulated solar wind electrons using truncated maxwellians, *Astron. Astrophys.*, **363**, 295, 2000.

Cranmer, S. R., Spectroscopic constraints on models of ion cyclotron resonance heating in the polar solar corona and high-speed solar wind, *J. Geophys. Res.*, **106**, 24937, 2001.

Cranmer, S. R., J. L. Kohl, and G. Noci, UVCS/SOHO: The first two years, *Space Sci. Rev.*, **85**, 341, 1998.

Cranmer, S. R., J. L. Kohl, G. Noci, et al., An empirical model of a polar coronal hole at solar minimum, *Astrophys. J.*, **511**, 481, 1999a.

Cranmer, S. R., G. B. Field, and J. L. Kohl, Spectroscopic constraints on models of ion cyclotron resonance heating in the polar solar corona and high-speed solar wind, *Astrophys. J.*, **518**, 937, 1999b.

Czechowski, A., R. Ratkiewicz, J. F. McKenzie, and W. I. Axford, Heating and acceleration of minor ions in the solar wind, *Astron. Astrophys.*, **335**, 303, 1998.

Denskat, K. U., and F. M. Neubauer, Statistical properties of low-frequency magnetic field fluctuations in the solar wind from 0.29 to 1.0 AU during solar minimum conditions: HELIOS 1 and HELIOS 2, *J. Geophys. Res.*, **87**, 2215, 1982.

Dusenbery, P. B., and J. V. Hollweg, Ion-cyclotron heating and acceleration of solar wind minor ions, *J. Geophys. Res.*, **86**, 153, 1981.

Feldman, W. C., B. L. Barraclough, J. L. Phillips, and Y.-M. Wang, Constraints on high-speed solar wind structure near its coronal base: a Ulysses perspective, *Astron. Astrophys.*, **316**, 355, 1996.

Fichtner, H., S. R. Sreenivasan, and N. Vormbrock, Transfer integrals for fully ionized gases, *J. Plasma Phys.*, **55**, 95, 1996.

Gary, S. P., B. E. Goldstein, and J. T. Steinberg, Helium ion acceleration and heating by Alfvén/cyclotron fluctuations in the solar wind, *J. Geophys. Res.*, **106**, 24955, 2001.

Hollweg, J. V., and J. M. Turner, Acceleration of solar wind He^{++} 3. Effects of resonant and nonresonant interactions with transverse waves, *J. Geophys. Res.*, **83**, 97, 1978.

Hu, Y. Q., and S. R. Habbal, Resonant acceleration and heating of solar wind ions by dispersive ion cyclotron waves, *J. Geophys. Res.*, **104**, 17045, 1999.

Hu, Y. Q., R. Esser, and S. R. Habbal, A fast solar wind model with anisotropic proton temperature, *J. Geophys. Res.*, **102**, 14661, 1997.

Ichimaru, S., *Basic Principles of Plasma Physics: A Statistical Approach*, W. A. Benjamin, Reading, Massachusetts, 1973.

Isenberg, P. A., Resonant acceleration and heating of solar wind ions: anisotropy and dispersion, *J. Geophys. Res.*, **89**, 6613, 1984.

Isenberg, P. A., M. A. Lee, and J. V. Hollweg, A kinetic model of coronal heating and acceleration by ion-cyclotron waves: preliminary results, *Solar Phys.*, **193**, 247, 2000.

Kohl, J. L., G. Noci, E. Antonucci, et al., UVCS/SOHO empirical determinations of anisotropic velocity distributions in the solar corona, *Astrophys. J.*, **501**, L127, 1998.

Leer, E., T. E. Holzer, and E. C. Shoub, Solar wind from a corona with a large helium abundance, *J. Geophys. Res.*, **97**, 8183, 1992.

Li, X., S. R. Habbal, J. V. Hollweg, and R. Esser, Heating and cooling of protons by turbulence-driven ion cyclotron waves in the fast solar wind, *J. Geophys. Res.*, **104**, 2521, 1999.

Liewer, P. C., M. Velli, and B. E. Goldstein, Alfvén wave propagation and ion cyclotron interactions in the expanding solar wind: One-dimensional hybrid simulations, *J. Geophys. Res.*, **1046**, 29261, 2001.

Maksimovic, M., V. Pierrard, and J. F. Lemaire, A kinetic model of the solar wind with Kappa distribution functions in the corona, *Astron. and Astrophys.*, **324**, 725, 1997.

Marsch, E., K.-H. Mühlhäuser, H. Rosenbauer, R. Schwenn, and F. M. Neubauer, Solar wind helium ions: observations of the Helios solar probes between 0.3 and 1 AU, *J. Geophys. Res.*, **87**, 35, 1982a.

Marsch, E., K.-H. Mühlhäuser, R. Schwenn, H. Rosenbauer, W. Pilipp, and F. M. Neubauer, Solar wind protons: three-dimensional velocity distributions and derived plasma parameters measured between 0.3 and 1 AU, *J. Geophys. Res.*, **87**, 52, 1982b.

Marsch, E., C. K. Goertz, and K. Richter, Wave heating and acceleration of solar wind ions by cyclotron resonance, *J. Geophys. Res.*, **87**, 5030, 1982c.

Olbert, S., Role of thermal conduction in the acceleration of the solar wind, *NASA Conf. Publ.*, 149, 1982.

Pierrard, V., M. Maksimovic, and J. F. Lemaire, Electron velocity distribution functions from the solar wind to the corona, *J. Geophys. Res.*, **104**, 17021, 1999.

Pilipp, W. G., H. Miggenrieder, K.-H. Mühlhäuser, H. Rosenbauer, and R. Schwenn, Large-scale variations of thermal electron parameters in the solar wind between 0.3 and 1 AU, *J. Geophys. Res.*, **95**, 6305, 1990.

Retterer, J. M., T. Chang, and J. R. Jasperse, Ion acceleration in the suprauroral region: a Monte Carlo model, *Geophys. Res. Lett.*, **10**, 583, 1983.

Schunk, R. W., Mathematical structure of transport equations for multispecies flows, *Rev. Geophys. Space Phys.*, **15**, 429, 1977.

Scime, E. E., S. J. Bame, W. C. Feldman, S. P. Gary, and J. L. Phillips, Regulation of the solar wind electrons heat flux from 1 to 5 AU: Ulysses observations, *J. Geophys. Res.*, **99**, 23401, 1994.

Scudder, J. D., and S. Olbert, A theory of local and global processes which affect solar wind electrons: 1. the origin of typical 1 AU velocity distribution functions — steady state theory, *J. Geophys. Res.*, **84**, 2755, 1979.

Steinberg, J. T., A. J. Lazarus, K. W. Ogilvie, R. Lepping, and J. Byrnes, Differential flow between solar wind protons and alpha particles: First WIND observations, *Geophys. Res. Lett.*, **23**, 1183, 1996.

Swanson, D. G., *Plasma Waves*, Academic Press, San Diego, CA, 1989.

Tam, S. W. Y., and T. Chang, Kinetic evolution and acceleration of the solar wind, *Geophys. Res. Lett.*, **26**, 3189, 1999a.

Tam, S. W. Y., and T. Chang, Solar wind acceleration, heating and evolution with wave-particle interactions, *Comments on Modern Phys.*, **1**, 141, 1999b.

Tam, S. W. Y., and T. Chang, Effect of electron resonant heating on the kinetic evolution and acceleration of the solar wind, *Geophys. Res. Lett.*, **28**, 1351, 2001.

Tam, S. W. Y., F. Yasseen, T. Chang, and S. B. Ganguli, Self-consistent kinetic photoelectron effects on the polar wind, *Geophys. Res. Lett.*, **22**, 2107, 1995.

Tam, S. W. Y., F. Yasseen, and T. Chang, Further development in theory/data closure of the photoelectron-driven polar wind and day-night transition of the outflow, *Ann. Geophys.*, **16**, 948, 1998.

Tu, C.-Y., and E. Marsch, Evidence for a "background" spectrum of solar wind turbulence in the inner heliosphere, *J. Geophys. Res.*, **95**, 4337, 1990.

Tu, C.-Y. On cyclotron wave heating and acceleration of solar wind ions in the outer corona, *J. Geophys. Res.*, **106**, 8233, 2001.

Vocks, C., and E. Marsch, A semi-kinetic model of wave-ion interaction in the solar corona, *Geophys. Res. Lett.*, **28**, 1917, 2001.

Vocks, C., and E. Marsch, Kinetic results for ions in the solar corona with wave-particle interactions and Coulomb collisions, *Astrophys. J.*, **568**, 1030, 2002.

IV. PUBLICATIONS:

- Chang, T., Complexity induced plasma turbulence in coronal holes and the solar wind, Solar Wind 10, to be published in 2003.
- Chang, T., S.W.Y. Tam, C.C. Wu, and G. Consolini, Complexity, forced and/or self-organized criticality, and topological phase transitions in space plasmas, Space Science Reviews, to be published in 2003.
- Chang, T. and C.C. Wu, "Complexity" and Anomalous Transport in Space Plasmas, Physics of Plasmas, 9, 3679, 2002.
- Chang, T., C.C. Wu, V. Angelopoulos, Preferential acceleration of coherent magnetic structures, bursty bulk flows (BBF), and intermittent turbulence in Earth's magnetotail, Physics Scripta, T98, 48, 2002.
- Tam, S.W.Y., and Tom Chang, Comparison of the effects of wave-particle interactions and the kinetic suprathermal electron population on the acceleration of the solar wind, Astron. and Astrophys., 395, 1001, 2002
- Tam, S.W.Y., and Tom Chang, Effect of electron resonant heating on the kinetic evolution and acceleration of the solar wind, Geophys. Res. Lett., 28, 1351, 2001.
- Chang, T., Colloid-like behavior and topological phase transitions in space plasmas: intermittent low frequency turbulence in the auroral zone, Physica Scripta, T89, 80, 2001.
- Chang, T., An example of resonances, coherent structures and topological phase transitions - The origin of the low frequency broad-band spectrum in the auroral zone, Nonlinear Processes in Geophysics, 8, 175, 2001.

- Consolini, G., and T. Chang, Magnetic field topology and criticality in geotail dynamics: relevance to substorm phenomena, Space Science Reviews, 95, 309, 2001
- Chang, T., S. Chapman, and A. Klimas, Forced and/or self-organized criticality (FSOC) in space plasmas, Journal of Atmospheric and Solar Terrestrial Physics, 63, 1359, 2001.
- Wu, C.C., and T. Chang, Further study of the dynamics of two-dimensional MHD coherent structures-- a large scale simulation, Journal of Atmospheric and Solar Terrestrial Physics, 63, 1447, 2001.
- Chapman, S.C., N.W. Watkins, and G. Rowlands, Signature of dual scaling regimes in a simple avalanche model for magnetospheric activity, Journal of Atmospheric and Solar Terrestrial Physics, 63, 1361, 2001.
- Consolini, G. and P. de Michelis, A revised forest-fire cellular automaton for the nonlinear dynamics of the Earth's magnetotail, Journal of Atmospheric and Solar Terrestrial Physics, 63, 1371, 2001.
- Wu, C. C., and T. Chang, 2D MHD simulation of the emergence and merging of coherent structures, Geophys. Res. Letters, 27, 863, 2000.
- Tam, Sunny W. Y., Tom Chang, S. C. Chapman, and N. W. Watkins, Analytical determination of power-law index for the Chapman et al. sandpile (FSOC) analog for magnetospheric activity -- a renormalization-group analysis, Geophys. Res. Lett., 27, 1367, 2000.

- Chang, T., Forced and/or self-organized criticality in space plasma processes, Physica Scripta, T84, 12, 2000.
- Tam, Sunny W.Y., and Tom Chang, Kinetic evolution and acceleration of the solar wind, Geophys. Res. Lett., 26. 3189, 1999.
- Chang, T., Self-organized criticality, multi-fractal spectra, sporadic localized reconnections and intermittent turbulence in the magnetotail, Physics of Plasmas, 5, 4137, 1999.
- Tam, Sunny W.Y., and Tom Chang, Solar wind acceleration, heating, and evolution with wave-particle interactions, Comments on Modern Physics, 1, 141, 1999.
- Chang, T., Self-organized criticality, multi-fractal spectra, and intermittent merging of coherent structures in the magnetotail, Astrophysics and Space Science, 264, 303, 1999.
- Chang, T., The role of coarse-grained helicity and self-organized criticality in magnetotail dynamics, in Magnetic Helicity in Space and Laboratory Plasmas, AGU Monograph Number 111, edited by M. R. Brown, R. C. Canfield and A. A. Pevtsov, p. 277 (American Geophysical Union, Washington, D.C., 1999).

SPECIAL ISSUES:

- T. Chang, S. Chapman, and A. Klimas (Editors), ``Forced and/or self-organized criticality (FSOC) in space plasmas," Journal of Atmospheric and Solar-Terrestrial Physics, , Elsevier, Netherlands, Volume 63(13), September 2001.

- Vassiliadis, D., Tom Chang, and S. Chapman, *Special Topics Section: Modes of Transport in Geospace*, (Guest Editors), Physics of Plasmas, 2002.
- Chang, Tom (Guest Editor), *Chandrasekhar Memorial Volume*, Int. J. Engng. Sci., 1999.

V. INVITED LECTURES:

- Symposium on Complexity in Space Plasma Processes, IUGG Assembly, Sapporo, Japan, 2003.
- Per Bak Memorial Session on Nonlinear Processes in Space Plasmas, Joint EGS-AGU-EUG Assembly, Nice, France, 2003.
- Session on Solar System Physics, Joint EGS-AGU-EUG Assembly, Nice, France, 2003.
- Triennial Tutorial Lecturer for the General Assembly of the International Union of Radio Science, Maastricht, Netherlands, 2002
- PARS (Polar Aeronomy and Radio Science) Workshop, Lake Arrowhead, CA, 2002.
- Huuntsville Workshop on Particle Acceleration in Space and Astrophysical Plasmas, Huntsville, TN, 2002.
- Eringem Symposium, Society of Engineering Science, State College, PA, 2002.
- International Workshop on Complexity in the Magnetotail Dynamics, Venice, Italy, 2002.
- International Topical Conference on Plasma Physics--New Plasma Horizons, Faro, Portugal, 2001.
- International Conference on Plasma Experiments in the Laboratory and in Space, IPELS--2001, Niseko, Hokkaido, Japan, 2001.
- International Workshop on Nonlinear Waves and Chaos in Space Plasmas, Tromso, Norway, 2001.

- Special Session on Reconnections at the American Geophysical Union Spring Meeting, Boston, MA, 2001.
- The 2001 US-Japan Workshop on Magnetic Reconnection, Princeton, N.J., 2001.
- Special Session on Solar Physics Plasmas, European Geophysical Union, Nice, France, 2001.
- Space Sciences Laboratory, University of California, Berkeley, CA, 2001.
- 33 COSPAR Assembly, Symposium on Alfvénic Structures: From the Sun to the Magnetosphere, Warsaw, Poland, 2000.
- International Conference on Colloidal Plasmas, Trieste, Italy, 2000.
- XXV General Assembly of the European Geophysical Society: Theory and Simulation on Solar System Plasmas, Nice, France, 2000.
- COSPAR Symposium on Space Weather Study Using Multi-Point Techniques, Taipei, Taiwan, 2000.
- American Physical Society Plasma Physics Mini-Symposium on Self-Organized Criticality and Turbulence, Seattle, WA, 1999.
- Goddard Space Flight Center, Series of Invited Tutorial Lectures on Forced and/or Self-Organized Criticality, Greenbelt, MD, 1999.
- International Topical Conference on Plasma Physics: New Frontiers of Nonlinear Sciences, Trieste, Italy, 1999.
- Kivelson Symposium, UCLA, Westwood, CA, 1999.

- Akebono Workshop on Auroral Plasma Dynamics: Akebono Ten Years Later, Banff, Canada, 1999.
- International Space Science Institute, Special Lecture on Self-Organized Criticality, Bern, Switzerland, 1999.
- IAGA Symposium on Turbulence and Solitary Structures in Space Plasmas: Theory, Experiments and Data Analyses, Birmingham, England, 1999.
- Self-Organized Criticality in Space Plasmas, Princeton Plasma Physics Laboratory, NJ, 1999.

VI. SCIENTISTS AND STUDENTS

Tom Chang, Director

Hannes Alfvén*, Nobel Laureate and Sponsor of Alfvén Lectureship (deceased)

W.T. Tam, Research Scientist

D. Tetreault, Research Scientist

Fareed Yasseen, Research Scientist and affiliate

Jay R. Johnson, Postdoctoral Associate

J.M. Retterer, Research Affiliate

J.R. Jasperse, Research Affiliate

James Ernstmeyer, Graduate Student

C.T. Dum, Research Affiliate

Andrew Yau, Visiting Scientist

Sandra Chapman, Visiting Scientist

Nick Watkins, Visiting Scientist

Kimani Stencil, Summer Minority Student Awardee

Vincenzo Vitelli, Visiting Student from Imperial College

Elese Archibald, Visiting Student from Imperial College

Iosif Bena, Undergraduate Research Opportunities Program Awardee

Toma Miloushev, Research Science Institute High School Intern

Wang Fei Cheang, Research Science Institute High School Intern